DESY 95--211
KA--TP--9--95
IFT--95--14

DESY 95–211
KA–TP–9–95
IFT–95–14
November 1995

hep-ph/9511342 16 Nov 1995

# Two– and Three–Body Decay Modes of SUSY Higgs Particles

A. Djouadi[1,2*], J. Kalinowski[3†] and P.M. Zerwas[2]

[1] Institut für Theoretische Physik, Universität Karlsruhe,
D–76128 Karlsruhe, FRG.

[2] Deutsches Elektronen–Synchrotron DESY, D–22603 Hamburg, FRG.

[3] Institute of Theoretical Physics, Warsaw University, PL–00681 Warsaw, Poland.

**Abstract**

We summarize the dominant decay modes of the neutral and charged Higgs bosons in the Minimal Supersymmetric extension of the Standard Model. While two–body decays are in general dominating, the branching ratios for three–body decays of the heavy scalar, pseudoscalar and charged Higgs bosons can be large below the thresholds if top quarks, $W/Z$ bosons or heavy scalar bosons are involved. Analytical expressions have been derived for the partial decay widths and the physical implications of these decay modes are discussed.

*Supported by Deutsche Forschungsgemeinschaft DFG (Bonn).
†Supported in part by a KBN grant.

## 1. Introduction

The experimental exploration of the electroweak gauge symmetry breaking is one of the most important tasks in particle physics. The observation of one or several fundamental scalar particles with couplings growing with the masses of the sources would establish the Higgs mechanism as the physical basis of the symmetry breaking. The Higgs mechanism [1] may be realized in the frame of the Standard Model ($\mathcal{SM}$) or one of its possible extensions among which supersymmetric theories are truly outstanding candidates [2, 3]. To explore the physical nature of the scalar particles, high-precision measurements of their properties are mandatory. To this end precise calculations of the production cross sections and the branching ratios of all important decay channels are required [4].

Since the Higgs couplings to the Standard Model particles are proportional to their masses [modulo enhancement/suppression factors in extended models] the most important decay channels are two–body decays to the heaviest particles allowed by phase space. Besides these two–body decays, below–threshold three–body decays of the Higgs bosons can also be very important. This is well-known in the Standard Model for Higgs decays to real and virtual pairs of $W/Z$ bosons in the intermediate mass range [5]: although suppressed by the off–shell propagator and the additional electroweak coupling between the $W/Z$ and the fermions, these decay processes are enhanced by the large Higgs couplings to the gauge bosons, giving rise to appreciable branching ratios.

In supersymmetric extensions of the Standard Model, below–threshold decays may become even more important, in particular for heavy Higgs decays to virtual and real gauge boson pairs, mixed gauge and Higgs boson pairs, as well as top quarks. The analysis of three–body decays of the Higgs bosons in the Minimal Supersymmetric Standard Model ($\mathcal{MSSM}$) has received not much attention in the literature so far. Only recently some below–threshold supersymmetric Higgs boson decays have been investigated numerically in Ref.[6]. We improve on this paper in several aspects: by performing the analysis analytically; by completing the ensemble of important decay channels; and last but not least, by studying the effects of stop mixing due to non–zero $\mathcal{SUSY}$ parameters $\mu$ and $A_t$. We will perform the analysis in the small and the large limit of tg$\beta$, the ratio of the vacuum expectation values, where the results for three–body decays turn out to be quite different. Both domains are interesting since they are realized in grand unified supersymmetric models with $b$–$\tau$ Yukawa coupling unification [7].

The paper is organized as follows. In the next Section, we summarize the main features of the Higgs sector in the $\mathcal{MSSM}$. In Section 3 we discuss the branching ratios in the large tg$\beta$ case, with special emphasis on decays for Higgs masses at the edge of the $\mathcal{SUSY}$ parameter space. In Section 4 we analyze the below-threshold decays of the heavy CP-even, CP-odd and charged Higgs bosons for small tg$\beta$ values. The total decay widths are summarized in Section 5. Supplementing analytical expressions will be presented in the Appendix.

## 2. Physical Set–Up

In the Minimal Supersymmetric extension of the Standard Model two isodoublets of Higgs fields [2] are introduced to provide masses to the up– and down–type fermions. This results in a spectrum of a quintet of physical particles: two CP–even neutral scalars $h$ and $H$, one CP–odd neutral (pseudo)scalar $A$, and a pair of charged scalar particles $H^{\pm}$. Besides the four masses, two additional parameters determine the properties of these particles at the tree level: the ratio tg$\beta$ of the vacuum expectation values of the two neutral Higgs fields and a mixing angle $\alpha$ in the neutral CP–even sector.

Supersymmetry leads to several relations among the parameters of the Higgs sector, and only two of them are in fact independent. If one of the Higgs boson masses [in general $M_A$] and tg$\beta$ are specified, all other masses and the mixing angle $\alpha$ can be derived at the tree–level [3]. Supersymmetry imposes a strong hierarchical structure on the mass spectrum, $M_h < M_A < M_H$, $M_W < M_{H^{\pm}}$ and $M_h < M_Z$, which however is broken by radiative corrections [8, 9].

The leading part of the radiative corrections grows as the fourth power of the top quark mass $m_t$ and the logarithm of the squark mass $M_S$ [8]. This part is determined by the parameter

$$\epsilon = \frac{3G_F}{\sqrt{2}\pi^2}\frac{m_t^4}{\sin^2\beta}\log\left(1+\frac{M_S^2}{m_t^2}\right) \tag{1}$$

These leading corrections can be summarized in a simple form [8]

$$\begin{aligned}
M_h^2 &= \frac{1}{2}\Big[M_A^2+M_Z^2+\epsilon \\
&\quad -\sqrt{(M_A^2+M_Z^2+\epsilon)^2-4M_A^2M_Z^2\cos^2 2\beta-4\epsilon(M_A^2\sin^2\beta+M_Z^2\cos^2\beta)}\Big] \\
M_H^2 &= M_A^2+M_Z^2-M_h^2+\epsilon \\
M_{H^{\pm}}^2 &= M_A^2+M_W^2 \qquad (2)\\
\mathrm{tg}2\alpha &= \mathrm{tg}2\beta\frac{M_A^2+M_Z^2}{M_A^2-M_Z^2+\epsilon/\cos 2\beta} \qquad \left[-\frac{\pi}{2}<\alpha<0\right] \qquad (3)
\end{aligned}$$

At the subleading level the radiative corrections are affected by the supersymmetric Higgs mass parameter $\mu$ and the parameter $A_t$ in the soft symmetry breaking interaction[1]. The radiative corrections are positive and they shift the mass of the light neutral Higgs boson $h$ upward. The variation of the Higgs boson masses $M_h$, $M_H$, $M_{H^{\pm}}$ with the pseudoscalar mass $M_A$ is shown in Fig. 1 for tg$\beta = 1.5$ and 30 in two mixing scenarios [10]: (i) (practically[2]) no mixing $\mu \ll M_S$, $A_t = 0$; and (ii) maximal mixing $\mu \ll M_S$, $A_t = \sqrt{6}M_S$. The top quark mass is fixed to $m_t = 175$ GeV and the scalar mass to $M_S = 1$

[1] We adopt the recent analysis of Ref.[10] where the full dependence on $\mu, A_t$ is taken into account and where the next–to–leading QCD corrections [9] are implemented.

[2] A value of $\mu \sim 100$ GeV is not experimentally excluded yet; the partial decay widths we are analyzing, change only slightly between $\mu = 0$ and 100 GeV.

TeV. If $M_A$ is large, the $A$, $H$, $H^\pm$ Higgs bosons are nearly degenerate while the lightest Higgs boson $h$ reaches its maximal mass value. Note that for small tg$\beta$ the ordering $M_H > M_{H^\pm} > M_A$ holds in the large mass range while $M_{H^\pm} > M_H \simeq M_A$ for large tg$\beta$ instead. The effect of non-zero $A_t$ and $\mu$ is quite significant since its shifts the maximal value of the $h$ mass upward by almost $\sim 20$ GeV; for large tg$\beta$ values, the relations $M_h \simeq M_A$, $M_H \simeq \max(M_h)$ for $M_A < \max(M_h)$ and $M_H \simeq M_A$, $M_h \simeq \max(M_h)$ for $M_A > \max(M_h)$, holding in the case of no mixing, still hold true when the mixing is included.

The couplings of the neutral Higgs bosons to fermions and gauge bosons depend on the angles $\alpha$ and $\beta$; they are given in Table 1 with the normalization defined by the $\mathcal{SM}$ couplings

$$g_{H_{\mathcal{SM}}ff} = \left[\sqrt{2}G_F\right]^{1/2} m_f \qquad \text{and} \quad g_{H_{\mathcal{SM}}VV} = 2\left[\sqrt{2}G_F\right]^{1/2} M_V^2 \tag{4}$$

The CP–even neutral Higgs bosons $h$, $H$ share the $\mathcal{SM}$ coupling to the massive gauge bosons, their couplings to down– (up–) type fermions are enhanced (suppressed) with respect to the $\mathcal{SM}$ case. If, in the case of large $A$ masses, the mass of the lightest Higgs boson is close to its upper limit for a given value of tg$\beta$, the couplings of $h$ to fermions and gauge bosons are $\mathcal{SM}$–like while the couplings of the heavy CP–even scalar $H$ are suppressed. The pseudoscalar Higgs boson has no tree-level couplings to gauge bosons; its couplings to down– (up)–type fermions are (inversely) proportional to tg$\beta$. Radiative corrections treated at the level discussed above, are incorporated in the mixing angle $\alpha$. The size of the couplings is shown in Fig. 2a for the mixing scenarios defined before. Here again, the mixing has a large impact; however the bulk of the effect consists of shifting the $h, H$ masses upward.

| $\Phi$ | $g_{\Phi \bar{u} u}$ | $g_{\Phi \bar{d} d}$ | $g_{\Phi VV}$ |
|---|---|---|---|
| $H_{\mathcal{SM}}$ | 1 | 1 | 1 |
| $h$ | $\cos\alpha/\sin\beta$ | $-\sin\alpha/\cos\beta$ | $\sin(\beta-\alpha)$ |
| $H$ | $\sin\alpha/\sin\beta$ | $\cos\alpha/\cos\beta$ | $\cos(\beta-\alpha)$ |
| $A$ | $1/\mathrm{tg}\beta$ | $\mathrm{tg}\beta$ | 0 |

Tab. 1: *Higgs boson couplings in the $\mathcal{MSSM}$ to fermions and gauge bosons relative to the $\mathcal{SM}$ Higgs couplings.*

In the limit of large $A, H$ masses, the $h$ mass becomes maximal. In this limit, the properties of $h$ approach those of the $\mathcal{SM}$ Higgs boson. The heavy neutral scalar Higgs boson $H$ decouples from the gauge bosons and the fermionic $H$ couplings approach the

corresponding couplings of the pseudoscalar Higgs boson $A$. For small $h, H$ masses, the light Higgs boson $h$ is built–up primarily by the Higgs field $H_2$ which couples to down–type fermions with the strength $\sim \mathrm{tg}\beta$, while the heavy Higgs boson $H$, built–up by $H_1$, couples conversely to up–type fermions.

For fermions the charged Higgs particles couple to mixtures of scalar and pseudoscalar currents, with components proportional to $m_u \mathrm{ctg}\beta$ and $m_d \mathrm{tg}\beta$ for the two $\pm$ chiralities,

$$g_{H^+ u\bar{d}} = \left(G_F/\sqrt{2}\right)^{1/2} [(1-\gamma_5) m_u \mathrm{ctg}\beta + (1+\gamma_5) m_d \mathrm{tg}\beta] \tag{5}$$

The couplings of two Higgs bosons with one gauge boson are listed in Table 2. They are normalized to the charged/neutral weak couplings

$$g_W = (\sqrt{2} G_F)^{1/2} M_W \quad \text{and} \quad g_Z = (\sqrt{2} G_F)^{1/2} M_Z \tag{6}$$

and they come with the sum of the Higgs momenta entering and leaving the vertices. Again, radiative corrections are incorporated in the mixing angle $\alpha$. The magnitude of these couplings can be read off Fig. 2a.

| $\Phi$ | $g_{\Phi AZ}/g_Z$ | $g_{\Phi H^\pm W^\pm}/g_W$ |
|---|---|---|
| $h$ | $\cos(\beta-\alpha)$ | $\mp\cos(\beta-\alpha)$ |
| $H$ | $-\sin(\beta-\alpha)$ | $\pm\sin(\beta-\alpha)$ |
| $A$ | 0 | 1 |

Tab. 2: *The couplings of two Higgs bosons with one gauge boson. They are normalized to the weak couplings defined in eq.(6) and they come with momenta of the Higgs particles entering and leaving the vertices.*

Finally, we summarize the couplings of the three neutral Higgs bosons among themselves which we will need in the subsequent analyses. Unlike the previous cases, the radiative corrections are not incorporated in the mixing angle $\alpha$ in total, but additional contributions must be taken into account explicitely. Normalized to

$$g'_Z = (\sqrt{2} G_F)^{1/2} M_Z^2 \tag{7}$$

the radiatively corrected self–couplings are to leading order [11]

$$\begin{aligned} \lambda_{Hhh} &= 2\sin 2\alpha \sin(\beta+\alpha) - \cos 2\alpha \cos(\beta+\alpha) + 3\frac{\epsilon}{M_Z^2}\frac{\sin\alpha}{\sin\beta}\cos^2\alpha \\ \lambda_{HAA} &= -\cos 2\beta \cos(\beta+\alpha) + \frac{\epsilon}{M_Z^2}\frac{\sin\alpha}{\sin\beta}\cos^2\beta \end{aligned} \tag{8}$$

These couplings are shown in Fig. 2b for the two mixing scenarios, including subleading contributions [10] for non–zero $\mu$ and $A_t$.

The value of tg$\beta$ determines to a large extent the decay pattern of the supersymmetric Higgs bosons. For large values of tg$\beta$ the pattern is simple, a result of the strong enhancement of the Higgs couplings to down–type fermions. The neutral Higgs bosons will decay into $b\bar{b}$ and $\tau^+\tau^-$ pairs, the charged Higgs bosons into $\tau\nu_\tau$ pairs below and $tb$ pairs above the top–bottom threshold. Only at the edges of the Higgs parameter space these simple rules are modified: If $h$ approaches the maximal mass value, the couplings become $\mathcal{SM}$–like and the decay modes follow the pattern of the Standard Model; if $H$ approaches the minimal mass value, it will mainly decay into $hh$ and $AA$ final states. The detailed analysis of the large tg$\beta$ scenario with special emphasis on

$$h \;\to\; W^*W^*, Z^*Z^* \to 4 \text{ fermions} \tag{9}$$

$$H \;\to\; hh^*, AA^* \to hb\bar{b}, Ab\bar{b} \tag{10}$$

is presented in Section 3.

For small values of tg$\beta \sim 1$ the decay pattern of the heavy neutral Higgs bosons is much more complicated [11, 12]. The $b$ decays are in general not dominant any more. Instead, cascade decays to pairs of light Higgs bosons and mixed pairs of Higgs and gauge bosons are important. Moreover, decays to gauge boson pairs play a major role. However, for very large masses, the neutral Higgs bosons decay almost exclusively to top quark pairs. The decay pattern of the charged Higgs bosons for small tg$\beta$ is similar to that at large tg$\beta$ except in the intermediate mass range where cascade decays to light Higgs and $W$ bosons are dominant for small tg$\beta$.

Besides these two–body decays, below–threshold three–body decays of Higgs bosons can play an important role. $\mathcal{SM}$ Higgs decays into real and virtual $Z$ pairs [5] provide the signature for searching these particles in the intermediate mass range at proton colliders. The suppression by the off–shell propagator and the additional electroweak coupling between the $Z$ boson and the fermions is at least partly compensated by the large Higgs coupling to the $Z$ bosons. By the same token, three–body decays of $\mathcal{MSSM}$ Higgs particles mediated by gauge bosons, heavy Higgs bosons and top quarks, are of physical interest, specifically, Fig. 3:

(i) heavy CP–even Higgs particle $H$:

$$H \;\to\; VV^* \to Vf\bar{f}^{(\prime)} \tag{11}$$

$$H \;\to\; AZ^* \to Af\bar{f} \tag{12}$$

$$H \;\to\; H^\pm W^{\mp *} \to H^\pm f\bar{f}' \tag{13}$$

$$H \;\to\; \bar{t}t^* \to \bar{t}bW^+ \tag{14}$$

(ii) CP–odd Higgs boson $A$:

$$A \;\to\; hZ^* \to hf\bar{f} \tag{15}$$

$$A \;\to\; \bar{t}t^* \to \bar{t}bW^+ \tag{16}$$

(iii) charged Higgs boson $H^\pm$:

$$H^\pm \;\to\; hW^* \;\to\; hf\bar{f}' \tag{17}$$
$$H^\pm \;\to\; AW^* \;\to\; Af\bar{f}' \tag{18}$$
$$H^\pm \;\to\; \bar{b}t^* \;\to\; \bar{b}bW \tag{19}$$

The decays $H \to W^+\bar{t}b$ can also be mediated by virtual $W^+H^{-*}$ and $W^+W^{-*}$ intermediate states, and likewise $A \to W^+\bar{t}b$ decays by $W^+H^{-*}$ states. However, these contributions, given in the Appendix, are very small. [Additional three–body decays, $H \to hh^*$ or $AA^*$ with $h^*, A^* \to b\bar{b}$, could be relevant only for $M_H$ a few hundred MeV from its minimum value if tg$\beta$ were very large.] Three–body decays of the light CP–even Higgs boson $h$ are negligible, with the only exception of $h \to W^*W^*$ for $M_h$ close to its maximal value.

The decay chains given in the listings above for the heavy Higgs bosons are the dominant mechanisms in the range of Higgs masses where multi–body decays are relevant. This may be exemplified for the first decay chain of $A$. In a microscopic analysis one would consider the chain $A \to h^*Z^* \to (b\bar{b})_h(f\bar{f})_Z$. However, for small values of tg$\beta$, the coupling $hbb$ is of order $\sqrt{G_F}m_b$ and much smaller than the gauge coupling $Zff$. As a result, the off–shell $h^*$ contributions are negligible compared to the off–shell $Z^*$ contributions below the two–particle threshold. The light Higgs boson $h$ can therefore be treated as a stable particle and the decay process can be described as a three–body process to a high level of accuracy. This feature enables us to approach the problem of below–threshold decays by simple analytical methods.

In the discussion so far we have disregarded Higgs decays to neutralinos, charginos and sfermions. Since we have assumed a common $\mathcal{SUSY}$ scale of order $M_S \sim 1$ TeV, decays to sfermions do not play a role in the Higgs mass range of a few hundred GeV which we are analyzing. If the chargino/neutralino channels are kinematically open, they affect the decay branching ratios in general very strongly [12]. Denoting the decay branching ratio without neutralino/chargino decays by $BR$ and the branching ratio for neutralino/chargino (and possibly sfermion) decays by $BR_\chi$, the finally observed branching ratio is given by

$$BR_{fin} = (1 - BR_\chi) \times BR \tag{20}$$

The branching ratios $BR_\chi$ depend on the supersymmetric Higgs parameter $\mu$ and the gaugino mass parameter $M_2$. For large values of $\mu$ and $M_2$, these decay modes can be neglected, yet for parameter sets $\mu \sim M_2 \sim \mathcal{O}(100)$ GeV, they could eventually dominate over all other decay modes [12]. Since the aim of the present paper is to identify the regions in the parameter space where the below–threshold decay modes might be important, we will assume, in the subsequent discussion, the decay channels to supersymmetric particles to be shut.

## 3. Higgs decay branching ratios: Large tg$\beta$

For large tg$\beta$ the Higgs couplings to down–type fermions dominate over all other couplings. As a result, the decay pattern is in general very simple. The neutral Higgs bosons will decay into $b\bar{b}$ and $\tau^+\tau^-$ pairs for which the branching ratios are close to $\sim 90$ % and $\sim 10$ %, respectively. In terms of the Fermi decay constant $G_F$, the partial decay widths into fermions are given by [3]

$$\Gamma(\Phi \to \bar{f}f) = N_c \frac{G_F M_\Phi}{4\sqrt{2}\pi} g^2_{\Phi ff} m_f^2 \beta^p \tag{21}$$

with $p = 3(1)$ for the CP–even (odd) Higgs bosons; $\beta = (1 - 4m_f^2/M_\Phi^2)^{1/2}$ is the velocity of the fermions in the final state, $N_c$ the color factor. The couplings $g_{\Phi ff}$ are collected in Table 1. For the decay widths into quark pairs, the QCD radiative corrections [13] are large and must be included. In the limit $M_\Phi \gg m_q$, the $\mathcal{O}(\alpha_s^2)$ corrected decay widths read [14]

$$\Gamma(\Phi \to q\bar{q}) = \frac{3G_F M_\Phi}{4\sqrt{2}\pi} m_q^2 g^2_{\Phi qq} \left[1 + 5.67 \left(\frac{\alpha_s}{\pi}\right) + (35.94 - 1.36N_F)\left(\frac{\alpha_s}{\pi}\right)^2\right] \tag{22}$$

with $\alpha_s \equiv \alpha_s(M_\Phi)$, $m_q^2 \equiv m_q^2(M_\Phi)$; $N_F = 5$ is the number of active quark flavors; all quantities are defined in the $\overline{\rm MS}$ scheme with $\Lambda^{(5)}_{\overline{\rm MS}} \sim 226$ MeV [which corresponds to the value $\alpha_s(M_Z^2) = 0.118$]. The bulk of these QCD corrections can be absorbed into running quark masses evaluated at the scale $\mu = M_\Phi$:

$$m_q(M_\Phi) = m_q(m_q) \left[\frac{\alpha_s(M_\Phi)}{\alpha_s(m_q)}\right]^{12/(33-2N_F)} \times \frac{1 + c_1^q \alpha_s(M_\Phi)/\pi + c_2^q \alpha_s^2(M_\Phi)/\pi^2}{1 + c_1^q \alpha_s(m_q)/\pi + c_2^q \alpha_s^2(m_q)/\pi^2} \tag{23}$$

In the case of bottom (charm) quarks, the coefficients are $c_1 = 1.17(1.01)$ and $c_2 = 1.50(1.39)$. For $M_\Phi \simeq 100$ GeV, the $b$ and $c$ quark masses $m_b(m_b) = 4.23$ and $m_c(m_c) = 1.23$ GeV, as extracted from QCD sum rules [15], have dropped to the effective values[3] $m_b(M_\Phi) \simeq 2.9$ GeV and $m_c(M_\Phi) \simeq 0.62$ GeV.

The charged Higgs particles decay into $\tau\nu_\tau$ pairs below and into $tb$ pairs above the top–bottom threshold. [Virtual $t^* \to bW$ contributions give rise to three–body decays for charged Higgs decays $H^\pm \to t^* b \to W b\bar{b}$ only a few GeV below the two-body decay threshold for $tb$ final states.] Neglecting one of the fermion masses in the phase space [$m_\nu = 0$ and $m_b \ll m_t$], the partial decay widths are [3]

$$\Gamma(H^+ \to u\bar{d}) = \frac{N_c G_F}{4\sqrt{2}\pi} M_{H^\pm} |V_{ud}|^2 \left(1 - \frac{m_f^2}{M_{H^\pm}^2}\right)^3 \left[m_d^2 {\rm tg}^2\beta + m_u^2 {\rm ctg}^2\beta - 4\frac{m_u^2 m_d^2}{M_{H^\pm}^2}\right] \tag{24}$$

with $V_{ud}$ being the CKM–like matrix element introduced for quark final states. Also in this case the QCD corrections [17] must be included. For light quarks, the bulk of these

[3] A detailed analysis of QCD effects in Higgs decays will be presented in Ref.[16].

corrections can be taken into account by using running quark masses; for the top quark, the QCD corrections are of order $\alpha_s/\pi$ and small, since the top quark mass is of the same order as the Higgs boson mass.

The branching ratios for these decays are shown in Fig. 4 for tg$\beta = 30$. Other decay modes become important only at the edges of the $\mathcal{SUSY}$ parameter space: (i) if $h$ approaches the maximum mass for a given value of tg$\beta$, and (ii) if $H$ approaches the minimum mass for a given value of tg$\beta$. These two cases are discussed below in detail.

### 3.1 The light neutral Higgs boson $h$

If the lightest CP–even Higgs boson $h$ approaches its maximum mass for a given value of tg$\beta$, the couplings become $\mathcal{SM}$–like and the decay pattern of the particles is the same as for the Higgs particle in the Standard Model. In this part of the parameter space, besides decays into charm quarks and gluons[4], neutral Higgs decays to pairs of real and virtual gauge bosons would be observed. Allowing both gauge bosons to be off–shell [important only for $h$ masses close to $M_W$ or $M_Z$], the partial decay width reads [19]

$$\Gamma(h \to V^* V^*) = \frac{1}{\pi^2} \int_0^{M_h^2} \frac{\mathrm{d}Q_1^2 M_V \Gamma_V}{(Q_1^2 - M_V^2)^2 + M_V^2 \Gamma_V^2} \int_0^{(M_h - Q_1)^2} \frac{\mathrm{d}Q_2^2 M_V \Gamma_V}{(Q_2^2 - M_V^2)^2 + M_V^2 \Gamma_V^2} \, \Gamma_0 \quad (25)$$

with $Q_1^2, Q_2^2$ being the squared invariant masses of the virtual gauge bosons, $M_V$ and $\Gamma_V$ their masses and total decay widths. $\Gamma_0$ is given by

$$\Gamma_0 = \frac{G_F M_h^3}{16\sqrt{2}\pi} \delta_V' \;\; \sin^2(\beta - \alpha) \lambda^{1/2}(Q_1^2, Q_2^2; M_h^2) \left[ \lambda(Q_1^2, Q_2^2; M_h^2) + \frac{12 Q_1^2 Q_2^2}{M_h^4} \right] \quad (26)$$

with $\delta_V' = 2(1)$ for $V = W(Z)$; $\lambda$ is the two–body phase space function defined by

$$\lambda(x, y; x) = (1 - x/z - y/z)^2 - 4xy/z^2 \quad (27)$$

The branching ratios for the lightest CP–even Higgs boson are shown as a function of $M_h$ near its maximal allowed mass value [in practice for $M_A = 1$ TeV] in Fig. 5a. The biggest uncertainty in the prediction of the decay branching ratios is associated with the badly known charm quark mass and the QCD coupling constant. To exemplify[5] the size of the uncertainty we have indicated the error of the branching ratio for $h \to c\bar{c}$ by the shaded band in Fig. 5a. The parameters chosen in the figure are the $\overline{\rm MS}$ QCD coupling $\alpha_s(M_Z^2) = 0.118 \pm 0.006$ and $m_c = 1.23 \pm 0.03$ GeV for the charm quark mass in the $\overline{\rm MS}$ scheme at the scale of the pole mass as extracted from QCD sum rules [15]. The partial charm decay width is calculated consistently to $\mathcal{O}(\alpha_s^2)$ with the renormalization scale set to the Higgs boson mass [16] (see also [20]). It is evident from Fig. 5a that the branching ratio for $h \to c\bar{c}$ is very uncertain. Since it is small, the migration of the error to the $b$ and $\tau$ branching ratios is less important, however.

[4]The expression for the gluonic decay width, including the QCD corrections, can be found in Ref.[18].

[5]We refrain from discussing the migration of the uncertainty in the charm sector to the other branching ratios which will be displayed in the figure for the central values of the coupling and mass parameters. A comprehensive discussion is presented in Ref.[16].

### 3.2 The heavy neutral Higgs boson $H$

If the mass of the heavy neutral CP–even Higgs boson is close to the minimal value [for tg$\beta \gg 1$, this corresponds to $M_A \simeq M_h < \mathcal{O}(100$ GeV)], the main decay modes are the cascade decays $H \to \Phi\Phi$ with $\Phi = h$ or $A$. For real light Higgs bosons, the partial decay widths are given by [3]

$$\Gamma(H \to \Phi\Phi) = \frac{G_F}{16\sqrt{2}\pi} \frac{M_Z^4}{M_H} \left(1 - 4\frac{M_\Phi^2}{M_H^2}\right)^{1/2} \lambda^2_{H\Phi\Phi} \tag{28}$$

where the radiatively corrected three–boson self–couplings have been given to leading order in eqs.(8,9) and including subleading terms in Fig. 2b. Since $M_h \simeq M_A$ and $\lambda_{Hhh} \simeq \lambda_{HAA}$ for large values of tg$\beta$, the two branching ratios are equal and close to 50% each. In this range of small $H$ masses, the decays $H \to \Phi\Phi^*$ with $\Phi^* \to b\bar{b}$, Fig. 3, can be important since the $\Phi bb$ coupling $\sim$ tg$\beta \gg 1$ is large. Taking into account only the diagrams where the $b\bar{b}$ final states originate from the decay of $h^*$ or $A^*$ [the additional channels where $h$ or $A$ are emitted from the $b$ lines in $H \to b\bar{b}$ give negligible contributions since the $Hbb$ coupling is very small in this mass range, see Fig. 2a], the Dalitz plot density for this three–body decay is given by

$$\frac{\mathrm{d}\Gamma}{\mathrm{d}x_1 \mathrm{d}x_2}(H \to \Phi\Phi^*) = K_{H\Phi\Phi} \frac{x_1 + x_2 - 1 + \kappa_\Phi}{(1 - x_1 - x_2)^2 + \kappa_\Phi \gamma_\Phi} \tag{29}$$

where $x_{1,2} = 2E_{1,2}/M_H$ are the scaled energies of the fermions in the final state [which we take to be massless], and $\kappa_\Phi = M_\Phi^2/M_H^2, \gamma_\Phi = \Gamma_\Phi^2/M_H^2$ for $\Phi = h, A$. The coefficient $K_{H\Phi\Phi}$ is given by

$$K_{H\Phi\Phi} = \frac{3G_F^2}{16\pi^3} \frac{M_Z^4}{M_H} g^2_{\Phi bb} m_b^2 \lambda^2_{H\Phi\Phi} \tag{30}$$

The integration of the Dalitz density over the energies $x_1$ and $x_2$ between the boundaries

$$\begin{aligned} 1 - x_2 - \kappa_\Phi < \quad x_1 \quad < 1 - \frac{\kappa_\Phi}{1 - x_2} \\ 0 < \quad x_2 \quad < 1 - \kappa_\Phi \end{aligned} \tag{31}$$

can be performed analytically, with the result for $M_H \lesssim 2M_\Phi - \Gamma_\Phi$ sufficiently below the thresholds

$$\begin{aligned} \Gamma(H \to \Phi\Phi^*) \;=\; & K_{H\Phi\Phi} \left[ (\kappa_\Phi - 1) \left(2 - \frac{1}{2}\log\kappa_\Phi\right) + \right. \\ & \left. \frac{1 - 5\kappa_\Phi}{\sqrt{4\kappa_\Phi - 1}} \left( \arctan \frac{2\kappa_\Phi - 1}{\sqrt{4\kappa_\Phi - 1}} - \arctan \frac{1}{\sqrt{4\kappa_\Phi - 1}} \right) \right] \end{aligned} \tag{32}$$

The branching ratios for these two decay modes are shown in Fig. 5b for tg$\beta = 30$ as a function of the pseudoscalar mass and for the two mixing scenarios discussed previously.

## 4. Higgs decay branching ratios: Small tg$\beta$

In the case tg$\beta \gtrsim 1$ the Higgs decay pattern is more complicated because the couplings to the light $b$ quarks and $\tau$ leptons are not enhanced any more and the couplings to the heavy top quark and the massive gauge bosons become increasingly important, leading in a natural way to a significant admixture of three–body decays.

### 4.1 The CP–even Higgs bosons

Even for small values of tg$\beta$, tg$\beta \gtrsim 1$, the light neutral CP-even Higgs boson $h$ decays primarily to $b$ quark and $\tau$ pairs. Only near its maximum mass limit, where the properties of $h$ are $\mathcal{SM}$–like, other decay modes become non–negligible, as discussed before. The branching ratios are shown in Fig. 6a for tg$\beta = 1.5$ in the cases of "no–mixing" and "maximal mixing" introduced above.

For the heavy neutral CP–even Higgs boson $H$, besides the usual 2–fermion $b\bar{b}$, $c\bar{c}$, $\tau\tau$ and the $gg$ decays, important channels are decays to pairs of light Higgs and gauge bosons and mixed pairs of Higgs and gauge bosons. Above the $t\bar{t}$ threshold, the Higgs boson $H$ decays almost exclusively to top quarks. We will concentrate on below–threshold 3–body decays involving gauge bosons, Higgs bosons and top quarks, Fig. 3.

*(i) Gauge boson pairs*

In the mass range above the $WW$ and $ZZ$ thresholds, where the $HVV$ couplings are not strongly suppressed for small values of tg$\beta$, the partial widths of the heavy Higgs particle $H$ for decays into massive gauge bosons may be written

$$\Gamma(H \to VV) = \frac{\sqrt{2} G_F M_H^3}{32\pi} \cos^2(\alpha-\beta)(1 - 4\kappa_V + 12\kappa_V^2)(1-4\kappa_V)^{1/2}\ \delta_V' \tag{33}$$

with $\kappa_V = M_V^2/M_H^2$ and $\delta_V' = 2(1)$ for $V = W(Z)$. Below the threshold for two real bosons, the decays to real and virtual $VV^*$ pairs are important down to Higgs masses $M_H \sim 130$ GeV. The Dalitz plot density for the decay process $H \to VV^* \to Vf\bar{f}^{(\prime)}$ is given by

$$\frac{\mathrm{d}\Gamma}{\mathrm{d}x_1 \mathrm{d}x_2}(H \to VV^*) = K_{HVV}\ \frac{(1-x_1)(1-x_2) + \kappa_V(2x_1 + 2x_2 - 3 + 2\kappa_V)}{(1-x_1-x_2)^2 + \kappa_V \gamma_V} \tag{34}$$

for all final $f\bar{f}'$ fermions taken massless [*i.e.* $t$ quark excluded] and summed up. The overall normalization factor $K_{HVV}$ is defined as

$$K_{HVV} = \frac{3 G_F^2 M_W^4}{16\pi^3} \cos^2(\beta-\alpha) M_H \delta_V \tag{35}$$

with

$$\delta_W = 3 \qquad \text{and} \quad \delta_Z = \frac{3}{c_W^4}\left(\frac{7}{12} - \frac{10}{9}s_W^2 + \frac{40}{27}s_W^4\right) \tag{36}$$

The factor $\gamma_V = \Gamma_V^2/M_H^2$ accounts for the non–zero width of the gauge boson $V$. The effect of the finite width is important in the threshold region since it guaranties the smooth transition from below– to above–threshold decays. Again, $x_i$ are the scaled energies of the fermions in the final state. The integration over the energies $x_1$ and $x_2$ between the boundaries in eq.(31) with $\kappa_\Phi$ replaced by $\kappa_V$, leads to the well–known result of Ref.[5] for the partial width $[M_H \lesssim 2M_V - \Gamma_V]$

$$\begin{aligned}\Gamma(H \to VV^*) &= K_{HVV} \left[\frac{1-8\kappa_V+20\kappa_V^2}{(4\kappa_V-1)^{1/2}} \arccos\left(\frac{3\kappa_V-1}{2\kappa_V^{3/2}}\right)\right. \\ &\left. -\frac{1-\kappa_V}{6\kappa_V}(2-13\kappa_V+47\kappa_V^2) - \frac{1}{2}(1-6\kappa_V+4\kappa_V^2)\log\kappa_V\right] \quad (37)\end{aligned}$$

*(ii) Cascade decays*

Potentially interesting decay modes are cascade decays of the heavy Higgs boson $H$ to mixed pairs of lighter Higgs bosons $h$, $A$ and gauge bosons, $H \to AZ$ and $H \to H^\pm W^\mp$. Because of the large value of the top quark mass the radiative corrections will shift the $H$ mass upward for a given value of $M_A$ or $M_{H^\pm}$ so that the phase space eventually opens for these decay modes. The partial decay widths for the two–body decays above threshold are given by the well-known expressions

$$\Gamma(H \to AZ) = \frac{G_F}{8\sqrt{2}\pi}\sin^2(\beta-\alpha)\,\frac{M_Z^4}{M_H}\lambda^{\frac{1}{2}}(M_A^2,M_Z^2;M_H^2)\lambda(M_A^2,M_H^2;M_Z^2) \quad (38)$$

$$\Gamma(H \to H^\pm W^\mp) = \frac{G_F}{8\sqrt{2}\pi}\sin^2(\beta-\alpha)\,\frac{M_W^4}{M_H}\lambda^{\frac{1}{2}}(M_{H^\pm}^2,M_W^2;M_H^2)\lambda(M_{H^\pm}^2,M_H^2;M_W^2) \quad (39)$$

with $\lambda$ being the two–body phase space function defined in eq.(27). Below–threshold decays of these modes are associated with virtual gauge boson decays to light fermions [$\neq t$, see later], $H \to AZ^* \to Af\bar{f}$ and $H \to H^\pm W^{\mp *} \to H^\pm f\bar{f}'$, cf. Fig. 3. In analogy to the gauge boson pair decays discussed in the previous paragraph, the Dalitz plot densities for the two processes may be written

$$\frac{\mathrm{d}\Gamma}{\mathrm{d}x_1\mathrm{d}x_2}(H \to AZ^* \to Af\bar{f}) = \frac{3G_F^2M_W^4}{8\pi^3}\sin^2(\alpha-\beta)M_H\delta_Z F_{AZ}(x_1,x_2) \quad (40)$$

$$\frac{\mathrm{d}\Gamma}{\mathrm{d}x_1\mathrm{d}x_2}(H \to H^\pm W^{\mp *} \to H^\pm f\bar{f}') = \frac{3G_F^2M_W^4}{8\pi^3}\sin^2(\alpha-\beta)M_H\delta_W F_{H^\pm W}(x_1,x_2) \quad (41)$$

where the density function $F_{ij}$ is given by

$$F_{ij}(x_1,x_2) = \frac{(1-x_1)(1-x_2)-\kappa_i}{(1-x_1-x_2-\kappa_i+\kappa_j)^2+\kappa_j\gamma_j} \quad (42)$$

Integrated over the Dalitz plots, the partial widths for decays sufficiently below the thresholds follow from

$$\Gamma(H \to AZ^* \to Af\bar{f}) = \frac{3G_F^2M_W^4}{8\pi^3}\sin^2(\alpha-\beta)M_H\delta_Z G_{AZ} \quad (43)$$

$$\Gamma(H \to H^\pm W^{\mp *} \to H^\pm f \bar{f}') \;=\; \frac{3G_F^2 M_W^4}{8\pi^3} \sin^2(\alpha-\beta) M_H \delta_W G_{H^\pm W} \tag{44}$$

with

$$G_{ij} = \frac{1}{4}\left\{ 2(-1+\kappa_j-\kappa_i)\sqrt{\lambda_{ij}}\left[\frac{\pi}{2} + \arctan\left(\frac{\kappa_j(1-\kappa_j+\kappa_i)-\lambda_{ij}}{(1-\kappa_i)\sqrt{\lambda_{ij}}}\right)\right]\right.$$
$$\left. +(\lambda_{ij}-2\kappa_i)\log(\kappa_i) + \frac{1}{3}(1-\kappa_i)\left[5(1+\kappa_i)-4\kappa_j-\frac{2}{\kappa_j}\lambda_{ij}\right]\right\} \tag{45}$$

and

$$\lambda_{ij} = -1+2\kappa_i+2\kappa_j-(\kappa_i-\kappa_j)^2 \tag{46}$$

*(iii) Top decays*

Another class of important decays involves the top quark. Above the top–quark threshold the partial decay width is given by

$$\Gamma(H \to \bar{t}t) \;=\; \frac{3G_F m_t^2}{4\sqrt{2}\pi}\, g_{Htt}^2\, M_H\, \beta_t^3 \tag{47}$$

with $\beta_t = (1-4m_t^2/M_H^2)^{1/2}$ being the velocity of the quarks in the final state; the coupling $g_{Htt} = \sin\alpha/\cos\beta$ has been discussed in the previous section [cf. Table 1 and Fig. 2a]. If the mass of the top quark in the Yukawa coupling is evaluated at the scale of the Higgs mass $m_t(M_H)$, the bulk of the QCD radiative corrections is effectively taken into account. Below the $tt$ threshold the final state $tbW$ can be reached through the $tt^*$ channel, Fig. 3. Since both the $W$ gauge boson mass and the top quark mass must be kept non–zero[6], the Dalitz plot density is more involved than in the previous cases. Using the more convenient variables $y_{1,2} = 1-x_{1,2}$, with $x_{1,2} = 2E_{t,b}/M_H$ for the reduced energies of the final top and bottom quarks, respectively, and the reduced masses $\kappa_i = M_i^2/M_H^2$, one obtains the Dalitz plot density

$$\frac{\mathrm{d}\Gamma}{\mathrm{d}x_1\mathrm{d}x_2}(H \to W^- t\bar{b}) = \frac{3G_F^2}{64\pi^3} m_t^2 M_H^3 \frac{\sin^2\alpha}{\sin^2\beta}\frac{\Gamma_0}{y_1^2+\gamma_t\kappa_t} \tag{48}$$

The amplitude squared $\Gamma_0$ is given by

$$\begin{aligned}\Gamma_0 \;=\;& y_1^2(1-y_1-y_2+\kappa_W-5\kappa_t)+2\kappa_W(y_1y_2-\kappa_W-2\kappa_t y_1+4\kappa_t\kappa_W)\\ & -\kappa_t y_1 y_2+\kappa_t(1-4\kappa_t)(2y_1+\kappa_W+\kappa_t)\end{aligned} \tag{49}$$

When performing the numerical integration over the energies $x_1, x_2$ of the Dalitz plot, bounded by

$$\left|\frac{2(1-x_1-x_2+\kappa_t+\kappa_b-\kappa_W)+x_1x_2}{\sqrt{x_1^2-4\kappa_t}\sqrt{x_2^2-4\kappa_b}}\right| \le 1 \tag{50}$$

[6]Since $m_b^2/M_H^2 \ll 1$, the $b$ quark mass can be neglected in the amplitude but we shall keep it non–zero in the phase space integration where its effect can be important.

to obtain the partial decay widths, the non–zero decay width of the virtual particles $\gamma_t = \Gamma_t^2/M_H^2$, as well as a non–zero value for $\kappa_b = m_b^2/M_H^2$, have been included. The charge conjugate $W^+\bar{t}b$ final state doubles the partial width.

Finally, partial widths for $H$ decays into two light Higgs bosons have to be included, see eq.(28). For small values of tg$\beta$, one needs to consider only the case where $\Phi = h, A$ are on–shell, since the $\Phi bb$ coupling is very small.

The branching ratios[7] for the main decay channels of the heavy Higgs boson $H$ are displayed in Fig. 6b for tg$\beta = 1.5$. Below the $t\bar{t}$ threshold, the decay $H \to hh$ is the dominant channel, superseded by decays to top quarks above the threshold. This rule is only broken for Higgs masses of about 140 GeV where an accidentally small value of the $\lambda_{Hhh}$ coupling allows the $b\bar{b}$ [no mix] and $WW^*$ [max mix] decay modes to become dominant. Important decay modes in general, below the $t\bar{t}$ threshold, are decays to pairs of gauge bosons, and $b\bar{b}$ decays. In a restricted range of the $H$ mass, also below–threshold $AZ^*$ and $H^\pm W^{\mp *}$ play a non–negligible role.

### 4.2 The pseudoscalar Higgs boson $A$

Since the pseudoscalar Higgs boson $A$ does not couple to pairs of $W$ and $Z$ bosons, the main two–body decay channels are $b\bar{b}$ and $\tau\tau$ decays and, in the mass range between about 150 GeV and 350 GeV, cascade decays to $hZ$ final states[8]. For small tg$\beta$, two–gluon decays are competitive in a limited Higgs mass range around 350 GeV.
*(i) Cascade decays*

Above the threshold, the partial width of the cascade decay $A \to hZ$ of the pseudoscalar Higgs boson reads

$$\Gamma(A \to hZ) = \frac{G_F}{8\sqrt{2}\pi} \cos^2(\beta-\alpha)\ \frac{M_Z^4}{M_A}\lambda^{1/2}(M_h^2, M_Z^2; M_A^2)\lambda(M_h^2, M_A^2; M_Z^2) \tag{51}$$

with $\lambda(x, y; z)$ being the two–body phase space function defined in eq.(27). The branching ratio is sizeable for masses between the $hZ$ and the $t\bar{t}$ thresholds for small values of tg$\beta$.

For $A$ masses below the threshold, three-body decays $A \to hZ^* \to hf\bar{f}$, mediated by virtual $Z$ bosons, can play a role, Fig. 3. In the same notation as before, the Dalitz plot density is given by

$$\frac{\mathrm{d}\Gamma}{\mathrm{d}x_1\mathrm{d}x_2}(A \to hZ^* \to hf\bar{f}) = \frac{3G_F^2 M_W^4}{8\pi^3} \cos^2(\alpha-\beta) M_A \delta_Z\ F_{hZ}(x_1, x_2) \tag{52}$$

with all possible $Z$ boson decays to light fermions summed up; the Dalitz plot function $F$ is given in eq.(42). Integrating out the energies $x_1$ and $x_2$ of the fermions, the partial

[7]The Fortran code for all partial decays widths of the $\mathcal{SM}$ and $\mathcal{MSSM}$ Higgs bosons may be obtained from djouadi@desy.de, jan.kalinowski@fuw.edu.pl or spira@desy.de.

[8]Since the pseudoscalar Higgs boson is always lighter than $H$ and $H^\pm$ in the $\mathcal{MSSM}$, the two–body decays $A \to HZ$ and $A \to H^\pm W^\mp$ are kinematically forbidden.

width of this decay process reads [$M_A < M_h + M_Z - \Gamma_Z$]

$$\Gamma(A \to hZ^* \to hf\bar{f}) = \frac{3G_F^2 M_W^4}{8\pi^3} \cos^2(\alpha-\beta) M_A \delta_Z G_{hZ} \tag{53}$$

with $G$ defined in eq.(45).

*(ii) Top decays*

The three–body process $A \to t\bar{b}W^-$, evolving out of the decay

$$\Gamma(A \to t\bar{t}) = \frac{3G_F m_t^2}{4\sqrt{2}\pi} g_{Att}^2 M_A \beta_t \tag{54}$$

is predominantly mediated by virtual $t$ quarks, $A \to t\bar{t}^*$ followed by $\bar{t}^* \to \bar{b}W^-$. Using the same notation as for the process $H \to t\bar{b}W^-$ we obtain for the Dalitz plot density

$$\frac{\mathrm{d}\Gamma}{\mathrm{d}x_1 \mathrm{d}x_2}(A \to t\bar{b}W^-) = \frac{3G_F^2 m_t^2 M_A^3}{64\pi^3 \mathrm{tg}^2\beta} \frac{\Gamma_0}{y_1^2 + \kappa_t \gamma_t} \tag{55}$$

with

$$\Gamma_0 = y_1^2(1 - y_1 - y_2 + \kappa_W - \kappa_t) + 2\kappa_W(y_1 y_2 - \kappa_W) - \kappa_t(y_1 y_2 - 2y_1 - \kappa_W - \kappa_t) \tag{56}$$

This reduced density approaches the corresponding expression for the scalar CP-even $H$ decay $H \to t\bar{b}W^-$ in the limit $M_{H,A} \gg m_t$ as expected from chiral symmetry. The non–zero width $\gamma_t = m_t^2/M_A^2$ of the top quark and the finite $b$–quark mass are taken into account when the Dalitz plot density is integrated out to obtain the partial width.

The numerical results for the two– and three–body decays of the pseudoscalar Higgs boson $A$ are summarized in Fig. 6c. The dominant modes are the $H \to b\bar{b}$ and $H \to t\bar{t}$ decays below the $hZ$ and $t\bar{t}$ thresholds respectively; in the intermediate mass region, $M_A = 200$ to 300 GeV, the decay $H \to AZ^*$ [which reaches the percent level already at $M_A = 130$ GeV] dominates. Note that this decay mode is more important in the case of no mixing. The gluonic decays are significant around the $t\bar{t}$ threshold.

### 4.3 The charged Higgs boson $H^\pm$

Except for the intermediate mass region, the main decay channels of the charged Higgs particles are the fermionic $\tau\nu_\tau$ and $tb$ modes. The bulk of the radiative QCD corrections can be taken into account by using running quark masses. Besides these channels, $H^+ \to c\bar{s}$ and $c\bar{b}$ modes are non–negligible, with the CKM–type suppression of the $cb$ current [$V_{cb} \sim 0.04$] partly compensated by the overall coupling $\sim m_b$ of this current.

*(i) Cascade decays*

If allowed kinematically, charged Higgs bosons can decay into the lightest neutral Higgs boson plus a $W$ boson

$$\Gamma(H^+ \to hW^-) = \frac{G_F \cos^2(\beta-\alpha)}{8\sqrt{2}\pi c_W^2} \frac{M_W^4}{M_{H^\pm}} \lambda^{\frac{1}{2}}(M_h^2, M_W^2; M_{H^\pm}^2) \lambda(M_h^2, M_{H^\pm}^2; M_W^2) \tag{57}$$

The branching ratio is quite substantial below the top threshold for small values of tg$\beta$ for which the $H^\pm W^\mp h$ coupling is not suppressed. The two–body decay of $H^+$ to $W^+A$ is kinematically not allowed.

There are three below–threshold decays of the charged Higgs boson with substantial branching ratios, two of which involve a virtual $W$ boson, $H^\pm \to hW^{\pm *} \to hf\bar{f}'$ and $H^\pm \to AW^{\pm *} \to Af\bar{f}'$, and one involves a virtual $t$ quark, $H^+ \to \bar{b}t^* \to \bar{b}bW^+$, Fig. 3.

The Dalitz plot densities involving the virtual $W$ boson are given by

$$\frac{\mathrm{d}\Gamma}{\mathrm{d}x_1 \mathrm{d}x_2}(H^+ \to hW^{+*} \to hf\bar{f}) = \frac{9G_F^2 M_W^4}{8\pi^3} \cos^2(\alpha-\beta) M_{H^\pm}\ F_{hW}(x_1, x_2) \tag{58}$$

$$\frac{\mathrm{d}\Gamma}{\mathrm{d}x_1 \mathrm{d}x_2}(H^+ \to AW^{+*} \to Af\bar{f}) = \frac{9G_F^2 M_W^4}{8\pi^3} M_{H^\pm}\ F_{AW}(x_1, x_2) \tag{59}$$

[$\kappa_i = M_i^2/M_{H^\pm}^2$ and $x_{1,2}$ being the energies of the $f\bar{f}$ final states], from which one obtains the partial decay widths below the thresholds

$$\Gamma(H^+ \to hW^{+*} \to hf\bar{f}) = \frac{9G_F^2 M_W^4}{8\pi^3} \cos^2(\alpha-\beta) M_{H^\pm}\ G_{hW} \tag{60}$$

$$\Gamma(H^+ \to AW^{+*} \to Af\bar{f}) = \frac{9G_F^2 M_W^4}{8\pi^3} M_{H^\pm}\ G_{AW} \tag{61}$$

The coefficients $F$ and $G$ have been defined in eqs.(42, 45).

*(ii) Top decays*

For the Dalitz plot density of the decay mode $H^+ \to \bar{b}t^* \to \bar{b}bW^+$, evolving out of

$$\Gamma(H^+ \to t\bar{b}) = \frac{3G_F}{4\sqrt{2}\pi} \frac{\lambda^{1/2}(t,b,H^\pm)}{M_{H^\pm}} |V_{tb}|^2 \times \Big[(M_{H^\pm}^2 - m_t^2 - m_b^2)\left(m_b^2 \mathrm{tg}^2\beta + m_t^2 \mathrm{ctg}^2\beta\right) - 4m_t^2 m_b^2\Big] \tag{62}$$

[with the CKM–type matrix element $V_{tb} \simeq 1$], we obtain

$$\frac{\mathrm{d}\Gamma}{\mathrm{d}x_1 \mathrm{d}x_2}(H^+ \to \bar{b}t^* \to Wb\bar{b}) = K_{H^\pm tb}\ \frac{(1-x_1)(1-x_2)/\kappa_W + 2x_1 + 2x_2 - 3 + 2\kappa_W}{(1-x_2-\kappa_t)^2 + \kappa_t\gamma_t} \tag{63}$$

with

$$K_{H^\pm tb} = \frac{3G_F^2 m_t^4}{32\pi^3} \frac{1}{\mathrm{tg}^2\beta}\ M_{H^\pm} \tag{64}$$

in the limit where the $b$ quark mass can be neglected; $x_{1,2} = 2E_{b,\bar{b}}/M_{H^\pm}$. Integrating out the energies of the Dalitz plot, the partial width [$M_{H^\pm} < m_t + m_b - \Gamma_t$] can be written as

$$\Gamma(H^\pm \to W b\bar{b}) = \frac{1}{2} K_{H^\pm tb} \left\{ \frac{\kappa_W^2}{\kappa_t^3}(4\kappa_W\kappa_t + 3\kappa_t - 4\kappa_W) \log \frac{\kappa_W(\kappa_t - 1)}{\kappa_t - \kappa_W} \right. \tag{65}$$
$$+(3\kappa_t^2 - 4\kappa_t - 3\kappa_W^2 + 1) \log \frac{\kappa_t - 1}{\kappa_t - \kappa_W} - \frac{5}{2}$$
$$\left. + \frac{1 - \kappa_W}{\kappa_t^2}(3\kappa_t^3 - \kappa_t\kappa_W - 2\kappa_t\kappa_W^2 + 4\kappa_W^2) + \kappa_W \left(4 - \frac{3}{2}\kappa_W\right) \right\}$$

The branching ratios of the most important two– and three–body decays, including the threshold effects in the numerical analysis, are displayed in Fig. 6d. The branching ratio is reduced for the $\tau\nu$ search channel of the charged Higgs boson quite significantly; indeed, by including of the three–body decays, this decay does not overwhelm all the other modes since the $H^+ \to hW^*$ channel as well the channels $H \to AW^*$ in the low mass range and $H^+ \to bt^*$ in the intermediate mass range, have appreciable branching ratios. [Here, as well as for the decay $A \to hZ^*$, we differ from Ref.[6].] It is interesting to observe that the mixing leads to a qualitative change of the decay pattern in the intermediate mass range: in the "no mixing" scenario the $hW^*$ decay mode is much more important than with mixing for moderately large charged Higgs masses.

## 5. Total widths of the Higgs particles

It is well known that the total widths of the $\mathcal{SUSY}$ Higgs particles are in general considerably smaller than the width of the $\mathcal{SM}$ Higgs particle.

The large width of the $\mathcal{SM}$ Higgs boson for high masses is due to the decays to longitudinal $W/Z$ bosons which grow as $G_F M_H^3$. The absence of the gauge boson couplings to $A$ and the decoupling from $H$ for large masses shut this channel. The dominant decay modes are built-up by top quarks so that the widths rise only linearly with the Higgs masses $\sim G_F m_t^2 M_H$. Detailed numbers are shown for the two different mixing scenarios in Fig. 7. While the width of the $\mathcal{SM}$ Higgs boson is of order $\Gamma_{H_{\mathcal{SM}}} \sim 200$ GeV for a Higgs mass $M_{H_{\mathcal{SM}}} \sim 750$ GeV, the width of the $\mathcal{SUSY}$ Higgs particles remain less than $\sim 10$ GeV in this mass range for moderate values of tg$\beta$.

For large tg$\beta$ values, the decay widths of all the five Higgs bosons are determined by $b$–quark finale states and they scale like tg$^2\beta$ [except for $h$ and $H$ near their maximal and minimal mass values, respectively]. The $H, A$ and $H^+$ widths therefore become experimentally significant, for tg$\beta$ values of order $\sim 50$ and above and for large Higgs masses [21].

**Acknowledgements**

Discussions with M. Spira are gratefully acknowledged. We thank S. Moretti and W.J. Stirling for a correspondence on pseudoscalar and charged Higgs decays. We also thank M. Carena for providing us with a Fortran code for Higgs masses and couplings in which the full dependence on the SUSY parameters $\mu$ and $A_t$ is taken into account. A.D. thanks the Theory Group for the warm hospitality extended to him at DESY.

# Appendix

Two of the three-body decays discussed before, $H \to tbW$ and $A \to tbW$, can be mediated by a superposition of different intermediate states. Even though these effects are rather small, they should nevertheless be given in this appendix for the sake of completeness. Omitting the finite decay widths of the virtual particles (which can easily be implemented) and using the notation introduced before, the Dalitz plot density may be written in the notation introduced before,

a) $\underline{H \to \bar{t}t^* + W^+H^{-*} + W^+W^{-*} \to W^+\bar{t}b:}$

$$\frac{\mathrm{d}\Gamma}{\mathrm{d}x_1\mathrm{d}x_2}(H \to W^-t\bar{b}) = \frac{3G_F^2}{64\pi^3}m_t^2M_H^3 \;\times \tag{A.1}$$
$$\left[\frac{\sin^2\alpha\;\Gamma_{11}}{\sin^2\beta\;y_1^2} + \frac{2\sin\alpha\sin(\beta-\alpha)\;\Gamma_{12}}{\sin\beta\mathrm{tg}\beta\;y_1(1-y_1-y_2+\kappa_W-\kappa_+)} + \frac{\sin^2(\beta-\alpha)\;\Gamma_{22}}{\mathrm{tg}^2\beta\;(1-y_1-y_2+\kappa_W-\kappa_+)^2}\right.$$
$$\left. + \frac{2\sin\alpha\cos(\beta-\alpha)\;\Gamma_{13}}{\sin\beta\;y_1(1-y_1-y_2)} + \frac{2\sin(\beta-\alpha)\cos(\beta-\alpha)\;\Gamma_{23}}{\mathrm{tg}\beta\;(1-y_1-y_2+\kappa_W-\kappa_+)(1-y_1-y_2)} + \frac{\cos^2(\beta-\alpha)\;\Gamma_{33}}{(1-y_1-y_2)^2}\right]$$

with the reduced amplitudes squared $\Gamma_{ii}$ and the interference terms $\Gamma_{ij}$ given by

$$\begin{aligned}
\Gamma_{11} &= y_1^2(1-y_1-y_2+\kappa_W-5\kappa_t) + 2\kappa_W(y_1y_2-\kappa_W) \\
&\quad +4\kappa_t(2\kappa_W^2-\kappa_W\kappa_t-\kappa_t^2-\kappa_W y_1-2y_1\kappa_t) + \kappa_t(2y_1-y_1y_2+\kappa_W+\kappa_t) \\
\Gamma_{12} &= (1-y_1-y_2+\kappa_W)(2\kappa_W-y_1^2-y_1y_2) + 2\kappa_t\kappa_W(y_2-y_1-3) \\
&\quad +\kappa_t(y_1+y_2)(3y_1+y_2-1+2\kappa_t) \\
\Gamma_{22} &= (y_1+y_2-1-\kappa_W+\kappa_t)\left[4\kappa_W-(y_1+y_2)^2\right] \\
\Gamma_{13} &= y_1^2(1-\kappa_W-y_1-y_2-2\kappa_t) + y_1y_2(1-y_1-y_2+3\kappa_W-4\kappa_t) \\
&\quad +2\kappa_W^2(4\kappa_W-2y_2-3y_1) + 2\kappa_W(y_2+y_1-1) \\
&\quad +\kappa_t\left[y_2(1-y_2-2\kappa_t)+y_1(1-y_1-2\kappa_t)-2\kappa_W(2\kappa_W+2\kappa_t+2y_1-3)\right]
\end{aligned}$$

$$
\begin{aligned}
\Gamma_{23} &= y_1^2(\kappa_W - 1 + y_1 + 3y_2 + \kappa_t) + y_2^2(-\kappa_W - 1 + y_2 + 3y_1 + \kappa_t) + 2y_1y_2\kappa_t \\
&\quad -2y_1y_2 + 2\kappa_W\left[y_2(\kappa_W - 2 + \kappa_t) + y_1(-\kappa_W - 2 + \kappa_t) + 2(1-\kappa_t)\right] \\
\Gamma_{33} &= 4\kappa_W^2\left[y_1y_2 + \kappa_W + 2\kappa_W(\kappa_W - y_1 - y_2)\right]/\kappa_t \\
&\quad +y_1^2(1 - \kappa_t - 3\kappa_W - y_1 - 3y_2) + y_2^2(1 - \kappa_t + \kappa_W - y_2 - 3y_1) \\
&\quad +2y_1y_2(1 - \kappa_t - \kappa_W) - 4\kappa_W\left[\kappa_W^2 + (\kappa_t - 1)(y_1 + y_2 - 1 + \kappa_W)\right]
\end{aligned} \tag{A.2}
$$

b) $\underline{A \to \bar{t}t^* + W^+H^{-*}W^{-*} \to W^+\bar{t}b:}$

$$
\begin{aligned}
\frac{\mathrm{d}\Gamma}{\mathrm{d}x_1\mathrm{d}x_2}(A \to W^-t\bar{b}) &= \frac{3G_F^2}{64\pi^3}\frac{m_t^2M_A^3}{\mathrm{tg}^2\beta} \times \\
&\quad \left[\frac{\Gamma_{11}}{y_1^2} + \frac{2\Gamma_{12}}{y_1(1 - y_1 - y_2 + \kappa_W - \kappa_+)} + \frac{\Gamma_{22}}{(1 - y_1 - y_2 + \kappa_W - \kappa_+)^2}\right]
\end{aligned} \tag{A.3}
$$

with the reduced amplitudes squared and the interference term

$$
\begin{aligned}
\Gamma_{11} &= y_1^2(1 - y_1 - y_2 + \kappa_W - \kappa_t) + 2\kappa_W(y_1y_2 - \kappa_W) - \kappa_t(y_1y_2 - 2y_1 - \kappa_W - \kappa_t) \\
\Gamma_{12} &= (1 - y_1 - y_2 + \kappa_W)(2\kappa_W - y_1^2 - y_1y_2) + \kappa_t[(y_1 + y_2)^2 - y_1 - y_2 - 2\kappa_W] \\
\Gamma_{22} &= (y_1 + y_2 - 1 - \kappa_W + \kappa_t)\left[4\kappa_W - (y_1 + y_2)^2\right]
\end{aligned} \tag{A.4}
$$

As expected from chiral symmetry, the expressions $\Gamma_{ij}$ approach the corresponding expressions for the decay $H \to t\bar{b}W$ in the limit $M_{H,A} \gg m_t$. Note that eqs.(A2) and (A4) are to be multiplied by a factor of 2 if the charge conjugate processes are taken into account.

# References


[1] P.W. Higgs, Phys. Rev. Lett. 12 (1964) 132, Phys. Rev. 145 (1966) 1156;
F. Englert and R. Brout, Phys. Rev. Lett. 13 (1964) 321;
G.S. Guralnik, C.R. Hagen and T.W. Kibble, Phys. Rev. Lett. 13 (1964) 585.

[2] P. Fayet, Nucl. Phys. B90 (1975) 104.

[3] For a review on the Higgs sector of the $\mathcal{MSSM}$, see J. Gunion, H. Haber, G. Kane and S. Dawson, The Higgs Hunter's Guide, Addison–Wesley, Reading 1990.

[4] P.M. Zerwas, Proceedings of the International Conference on High–Energy Physics, Marseille, 1993;
A. Djouadi, Int. J. Mode. Phys. A10 (1995) 1.

[5] T.G. Rizzo, Phys. Rev. D22 (1980) 389;
W.-Y. Keung and W.J. Marciano, Phys. Rev. D30 (1984) 248.

[6] S. Moretti and W. J. Stirling, Phys. Lett. B347 (1995) 291 and *erratum*.

[7] M. Carena, S. Pokorski and C.E.M. Wagner, Nucl. Phys. B406 (1993) 59;
M. Berger, V. Barger and P. Ohmann, Phys. Rev. D47 (1993) 1093.

[8] Y. Okada, M. Yamaguchi and T. Yanagida, Prog. Theor. Phys. 85 (1991) 1;
H. Haber and R. Hempfling, Phys. Rev. Lett. 66 (1991) 1815;
J. Ellis, G. Ridolfi and F. Zwirner, Phys. Lett. 257B (1991) 83.

[9] R. Hempfling and A. Hoang, Phys. Lett. B331 (1994) 99;
J. Casas, J. Espinosa, M. Quiros and A. Riotto, Nucl. Phys. B436 (1995) 3.

[10] M. Carena, J. Espinosa, M. Quiros and C. Wagner, Phys. Lett. B355 (1995) 209.

[11] V. Barger, M. Berger, A. Stange and R. Phillips, Phys. Rev. D45 (1992) 4128;
Z. Kunszt and F. Zwirner, Nucl. Phys. B385 (1992) 3.

[12] A. Djouadi, J. Kalinowski and P. M. Zerwas, Z. Phys. C57 (1993) 565.

[13] E. Braaten and J. P. Leveille, Phys. Rev. D22 (1980) 715;
M. Drees and K. Hikasa, Phys. Lett. B240 (1990).

[14] S. Gorishny, A. Kataev, S. Larin and L. Surguladze, Mod. Phys. Lett. A5 (1990) 2703.

[15] S. Narison, Phys. Lett. B341 (1994) 73.

[16] A. Djouadi, M. Spira and P.M. Zerwas, DESY Report 95–210.

[17] A. Mendez and A. Pomarol, Phys. Lett. B252 (1990) 461;
A. Djouadi and P. Gambino, Phys. Rev. D51 (1995) 218.

[18] A. Djouadi, M. Spira and P.M. Zerwas, Phys. Lett. B264 (1991) 440;
M. Spira, A. Djouadi, D. Graudenz and P.M. Zerwas, Nucl. Phys. B453 (1995) 17.

[19] R. N. Cahn, Rep. Prog. Phys. 52 (1989) 389.

[20] E. Gross, B. Kniehl and G. Wolf, Z. Phys. C63 (1994) 417, (E) C66 (1995) 321.

[21] P. Janot et al., ALEPH Collab., Report EPS0415, Proceedings of the International Conference on High–Energy Physics, Brussels 1995.

# Figure Captions

**Fig. 1:** The masses of the $\mathcal{MSSM}$ neutral CP–even Higgs bosons $h, H$ and the charged Higgs boson $H^\pm$ as a function of the pseudoscalar $A$ mass for two values of tg$\beta = 1.5$ (solid lines) and tg$\beta = 30$ (dashed lines); the long-dashed line presents $M_{H^\pm}$. a) "no mixing": $A_t = 0$, $\mu = 100$ GeV and $M_S = 1$ TeV, and b) "maximal mixing": $A_t = \sqrt{6} M_S, \mu = \ll M_S$ and $M_S = 1$ TeV. [$M_{H^\pm}$ does not depend on the mixing.]

**Fig. 2a:** The coupling parameters of the neutral CP–even Higgs bosons to fermions and gauge bosons as functions of the Higgs masses for the two values tg$\beta = 1.5$ and 30; no mixing (solid lines) and maximal mixing (dashed lines). The couplings are normalized to the $\mathcal{SM}$ couplings as defined in Table 1.

**Fig. 2b:** The trilinear couplings of the $\mathcal{MSSM}$ heavy neutral CP–even Higgs boson. (i) $\lambda_{Hhh}$ and (ii) $\lambda_{HAA}$ as functions of the $H$ mass for the two values tg$\beta = 1.5$ and 30; no mixing (solid lines) and maximal mixing (dashed lines).

**Fig. 3:** Main mechanisms for below–threshold three–body $\mathcal{MSSM}$ Higgs decays.

**Fig. 4:** The branching ratios of the $\mathcal{MSSM}$ Higgs bosons $h$, $H$, $A$ and $H^\pm$ as functions of their masses for tg$\beta = 30$; no mixing (solid lines) and maximal mixing (dashed lines). For the pseudoscalar and charged Higgs bosons the two mixing scenarios are indistinguishable in this case.

**Fig. 5a:** The branching ratios of the light CP–even $\mathcal{MSSM}$ Higgs boson $h$ as a function of its maximum mass value for the two mixing scenarios. The dashed band attached to the charm branching ratio, indicates the QCD uncertainties.

**Fig. 5b:** The branching ratios of the heavy CP–even $\mathcal{MSSM}$ Higgs boson $H$ near its minimum mass value as a function of $M_A$ for tg$\beta = 30$ and for the two mixing scenarios.

**Fig. 6a:** The branching ratios of the light CP–even $\mathcal{MSSM}$ Higgs boson $h$ for tg$\beta = 1.5$.

**Fig. 6b:** The branching ratios of the heavy CP–even $\mathcal{MSSM}$ Higgs boson $H$ for tg$\beta = 1.5$.

**Fig. 6c:** The branching ratios of the CP–odd $\mathcal{MSSM}$ Higgs boson $A$ for tg$\beta = 1.5$; (i) no mixing and (ii) maximal mixing.

**Fig. 6d:** The branching ratios of the $\mathcal{MSSM}$ charged Higgs boson $H^\pm$ for tg$\beta = 1.5$; (i) no mixing and (ii) maximal mixing.

**Fig. 7:** The total widths of the four $\mathcal{MSSM}$ Higgs bosons $h, H, A$ and $H^\pm$ as functions of the pseudoscalar mass $M_A$ for the two values tg$\beta = 1.5$ and 30/50 and the two scenarios of "no mixing" and "maximal mixing".

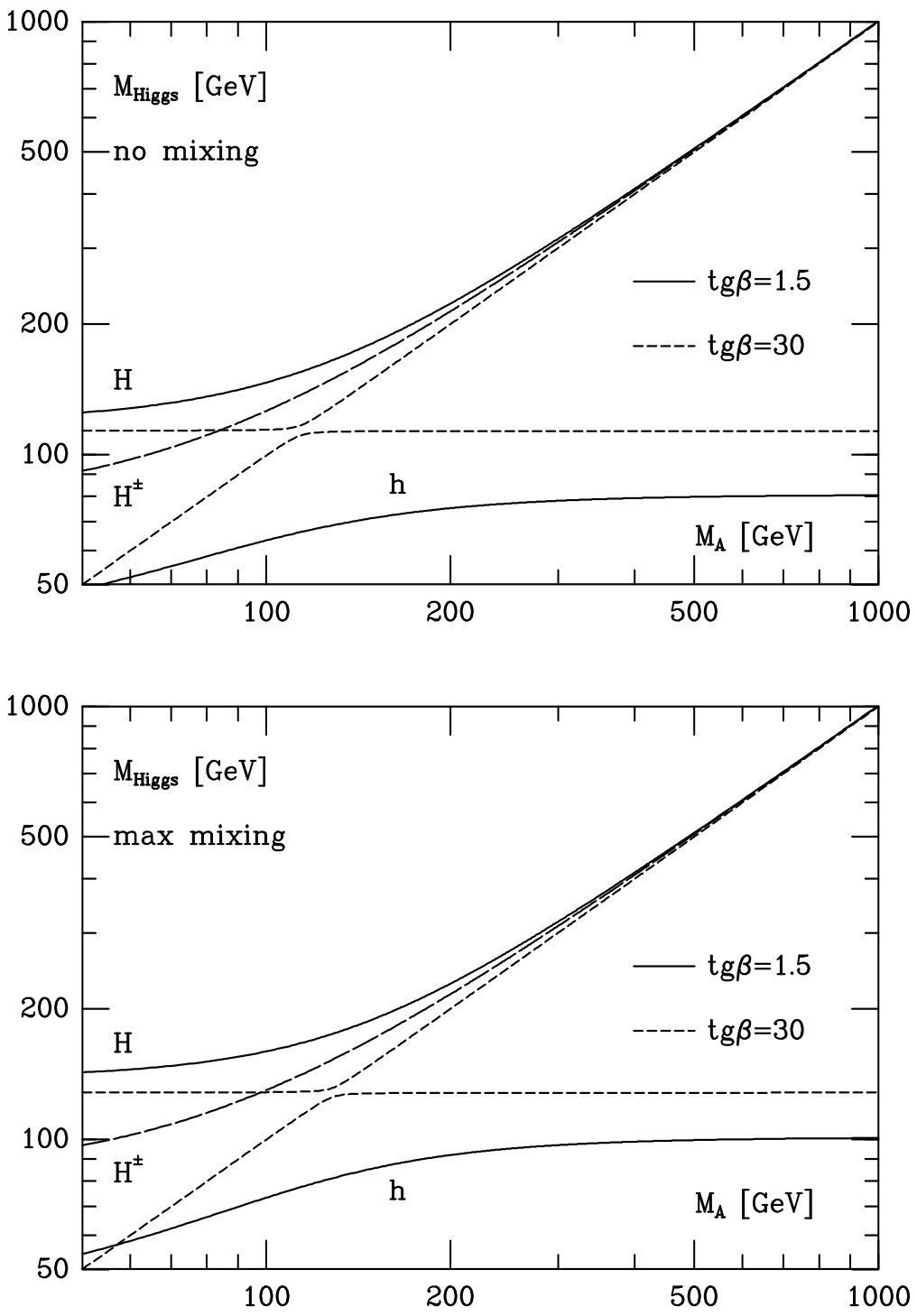
1000
500
200
100
50
$M_{Higgs}$ [GeV]
no mixing
tgβ=1.5
tgβ=30
H
$H^{\pm}$
h
$M_A$ [GeV]
100
200
500
1000
1000
500
200
100
50
$M_{Higgs}$ [GeV]
max mixing
tgβ=1.5
tgβ=30
H
$H^{\pm}$
h
$M_A$ [GeV]
100
200
500
1000

Fig. 1

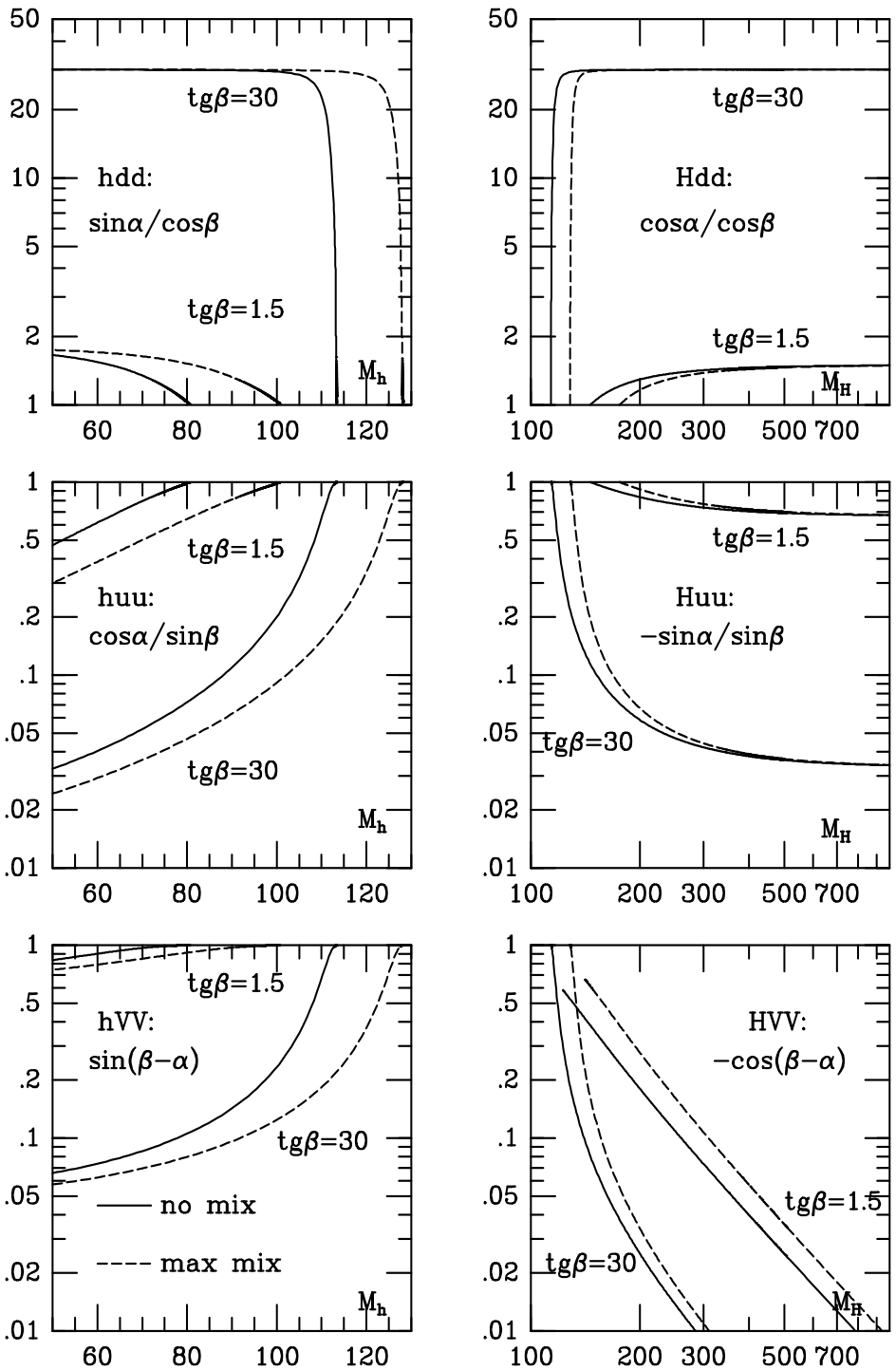
tgβ=30
hdd:
sinα/cosβ
tgβ=1.5
M_h
Hdd:
cosα/cosβ
M_H
huu:
cosα/sinβ
Huu:
−sinα/sinβ
hVV:
sin(β−α)
HVV:
−cos(β−α)
no mix
max mix

Fig. 2a

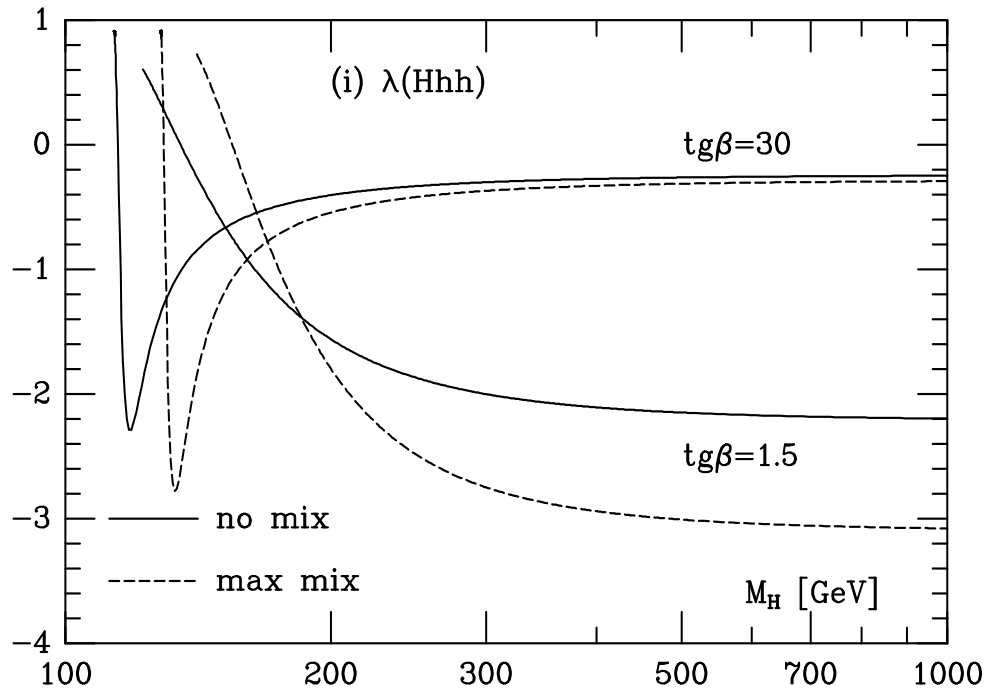
(i) λ(Hhh)
tgβ=30
tgβ=1.5
no mix
max mix
M_H [GeV]
1
0
−1
−2
−3
−4
100
200
300
500
700
1000

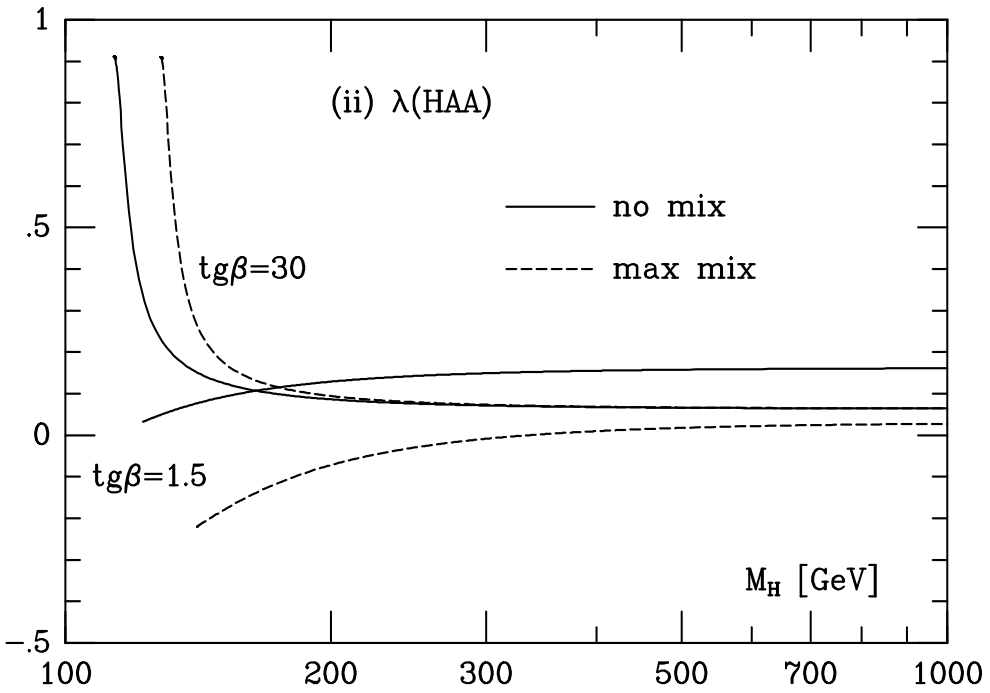
(ii) λ(HAA)
no mix
max mix
tgβ=30
tgβ=1.5
M_H [GeV]
1
.5
0
−.5
100
200
300
500
700
1000

**Fig. 2b**

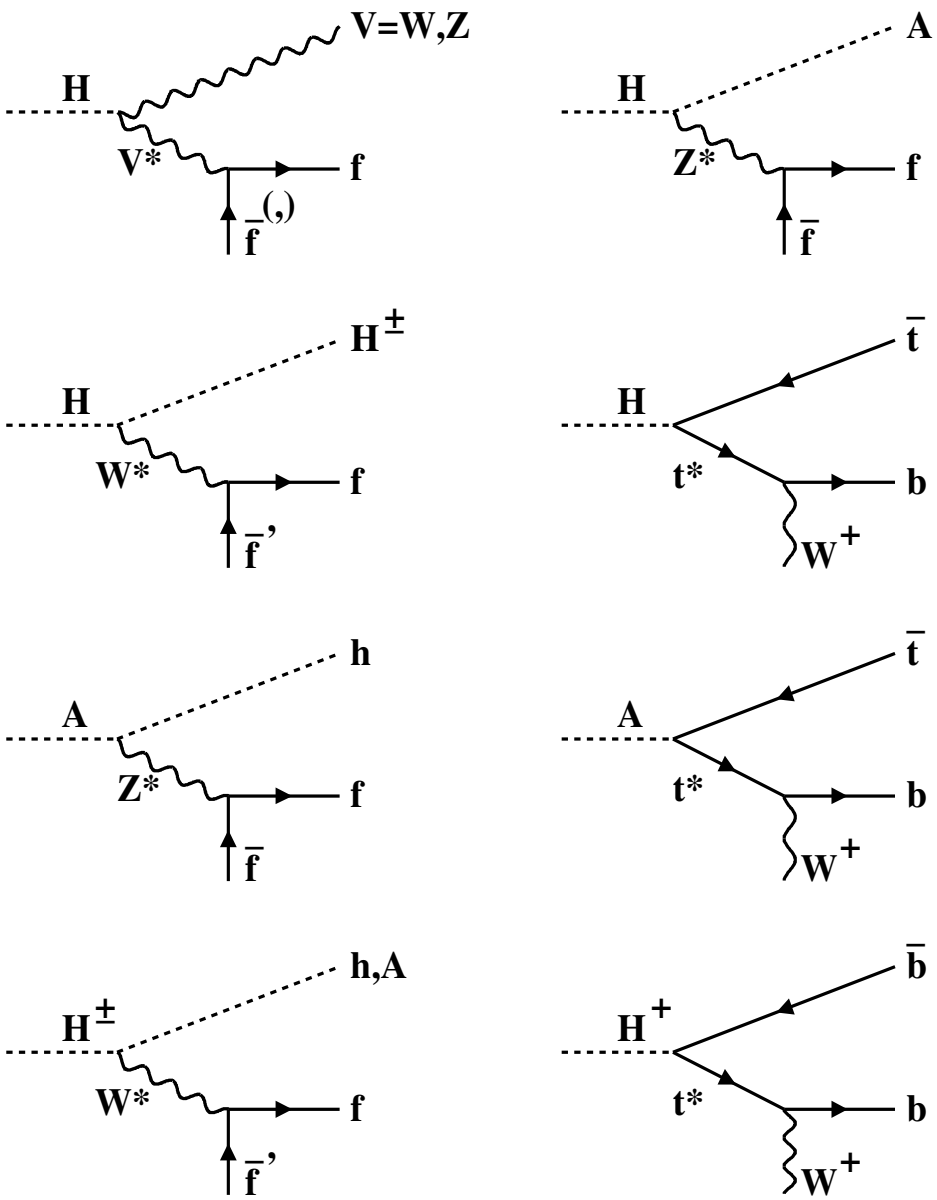


**Fig.3**

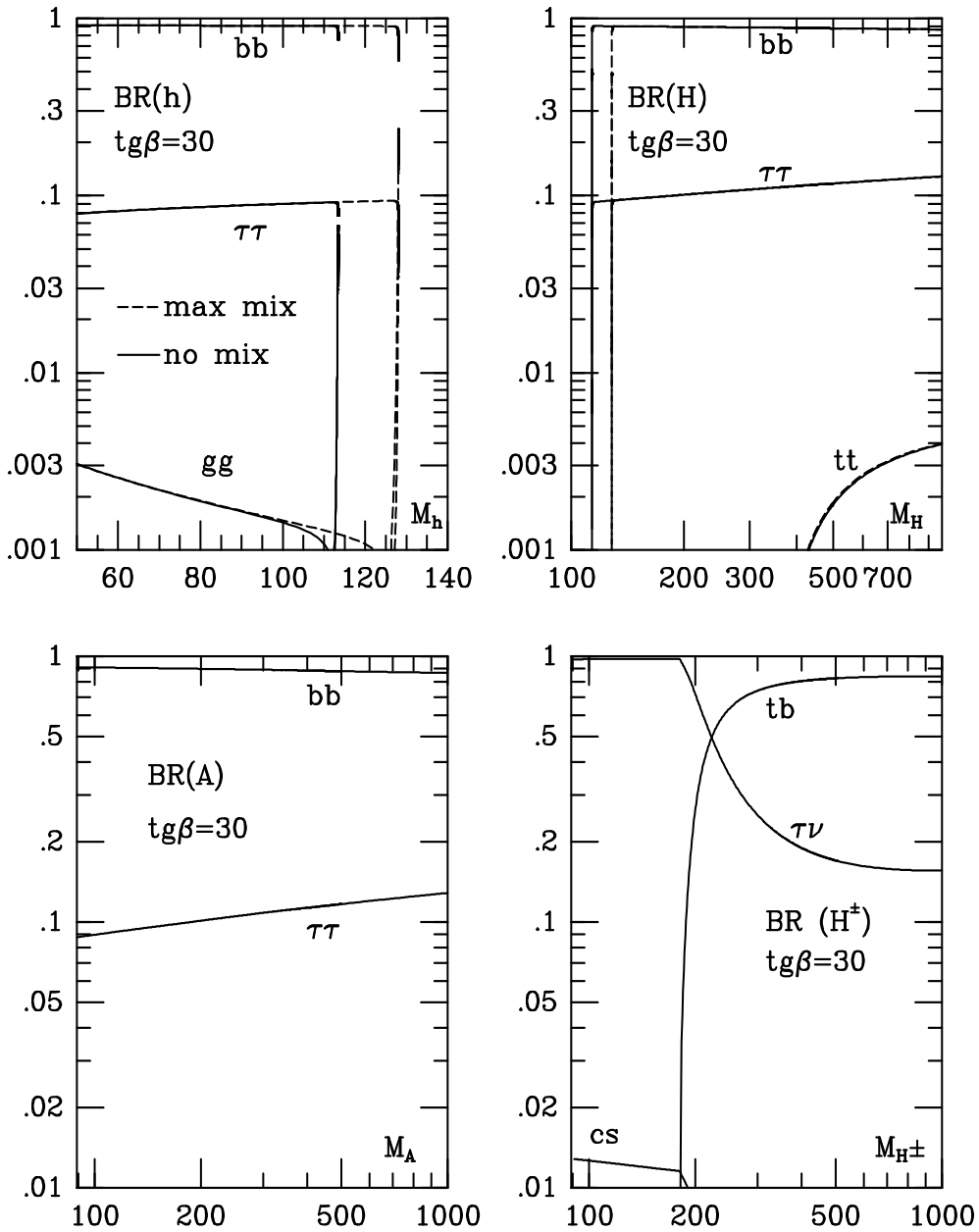
BR(h)
tgβ=30
bb
ττ
---max mix
——no mix
gg
M_h
BR(H)
tgβ=30
bb
ττ
tt
M_H
BR(A)
tgβ=30
bb
ττ
M_A
BR (H±)
tgβ=30
tb
τν
cs
M_H±

Fig. 4

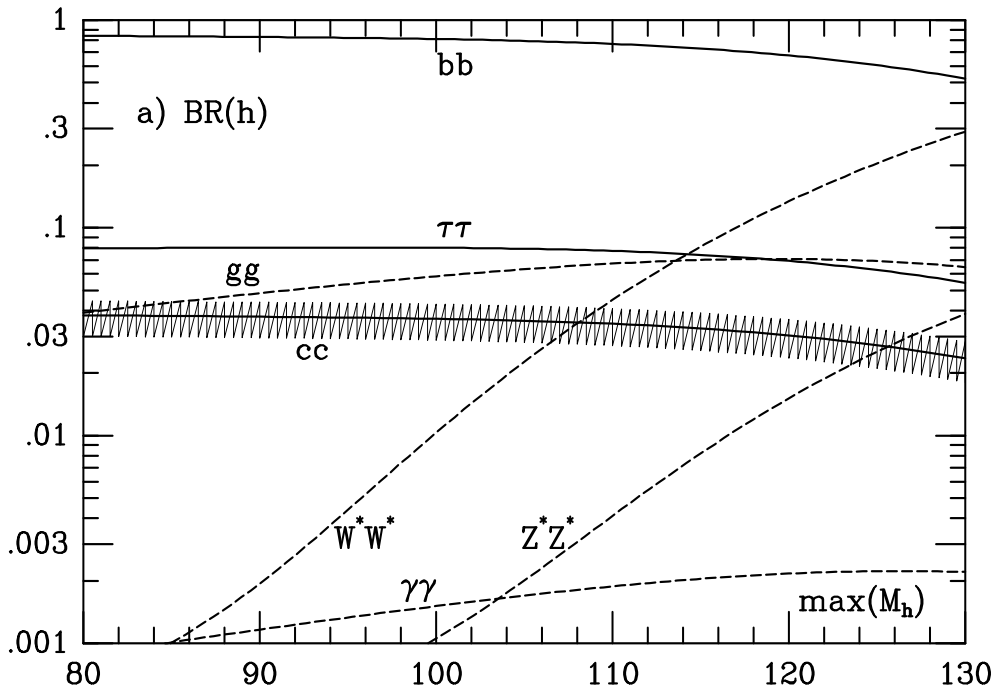
a) BR(h)
bb
ττ
gg
cc
W*W*
Z*Z*
γγ
max(M_h)
1
.3
.1
.03
.01
.003
.001
80
90
100
110
120
130

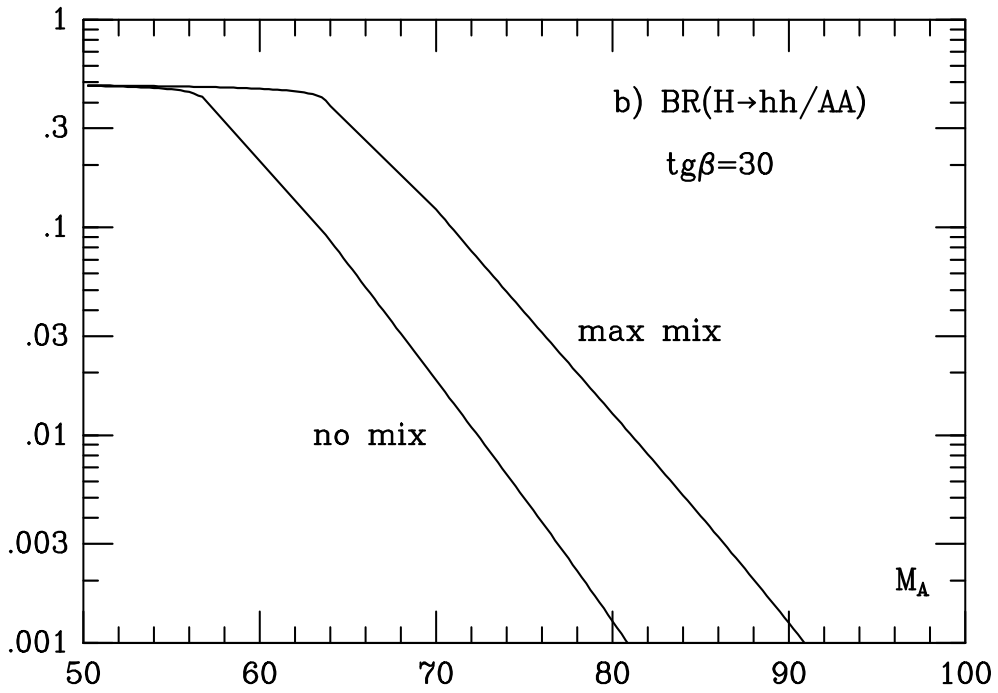
b) BR(H→hh/AA)
tgβ=30
max mix
no mix
M_A
1
.3
.1
.03
.01
.003
.001
50
60
70
80
90
100

**Fig. 5**

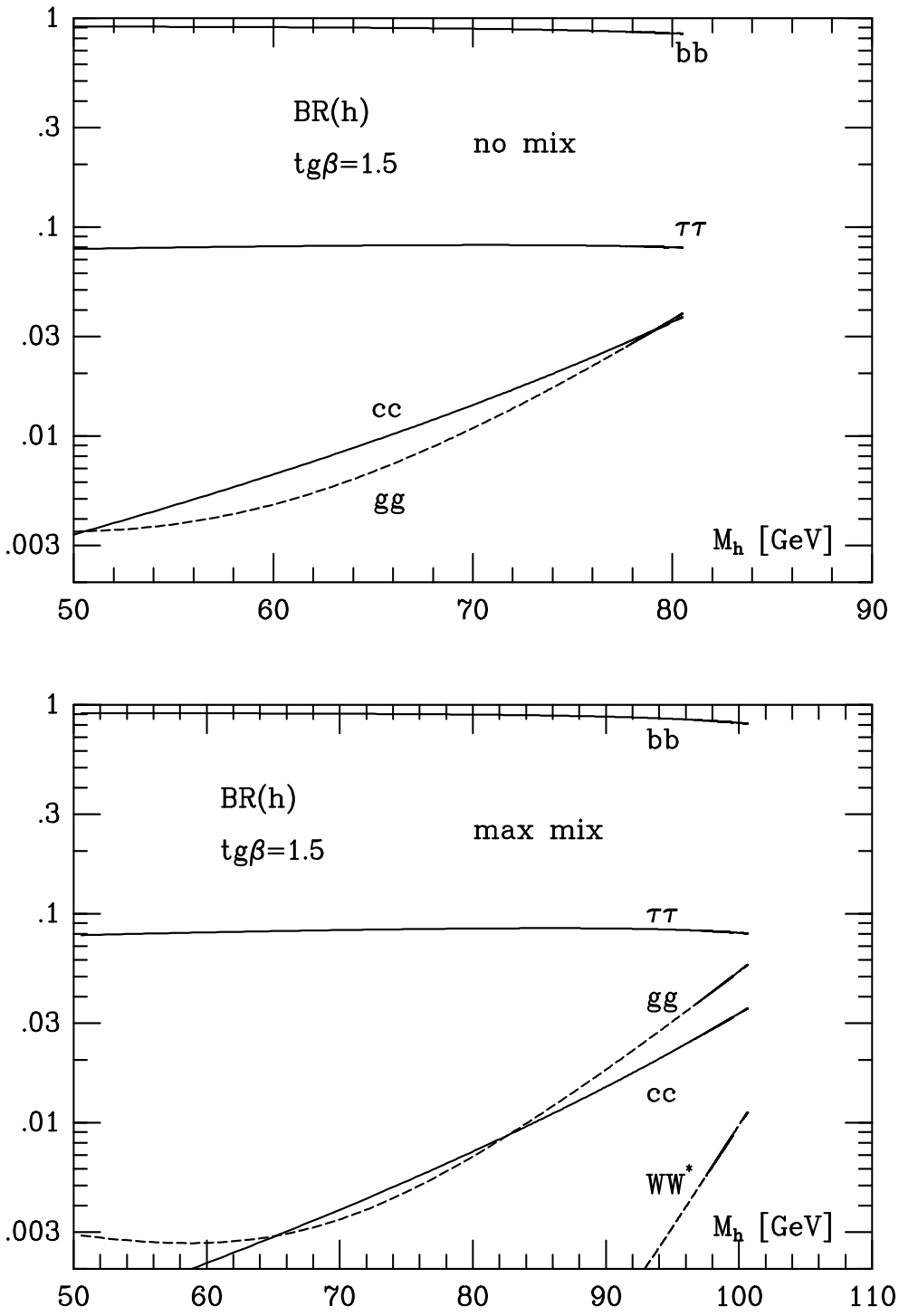
1
.3
.1
.03
.01
.003
BR(h)
tgβ=1.5
no mix
bb
ττ
cc
gg
M_h [GeV]
50
60
70
80
90
BR(h)
tgβ=1.5
max mix
bb
ττ
gg
cc
WW*
M_h [GeV]
50
60
70
80
90
100
110

Fig. 6a

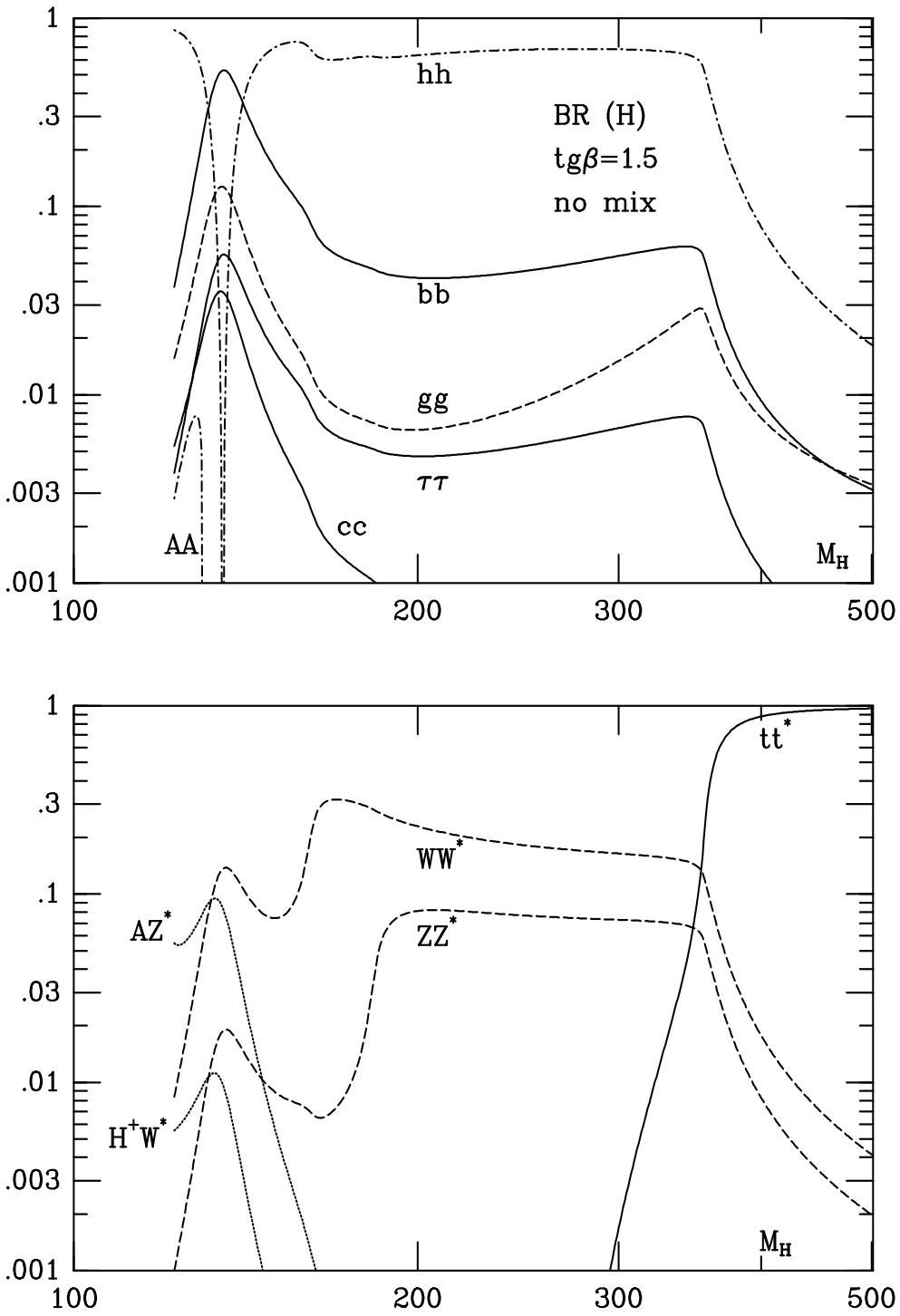
1
.3
.1
.03
.01
.003
.001
100
200
300
500
hh
BR (H)
tgβ=1.5
no mix
bb
gg
ττ
cc
AA
M_H
1
.3
.1
.03
.01
.003
.001
100
200
300
500
tt*
WW*
AZ*
ZZ*
H+W*
M_H

Fig. 6b

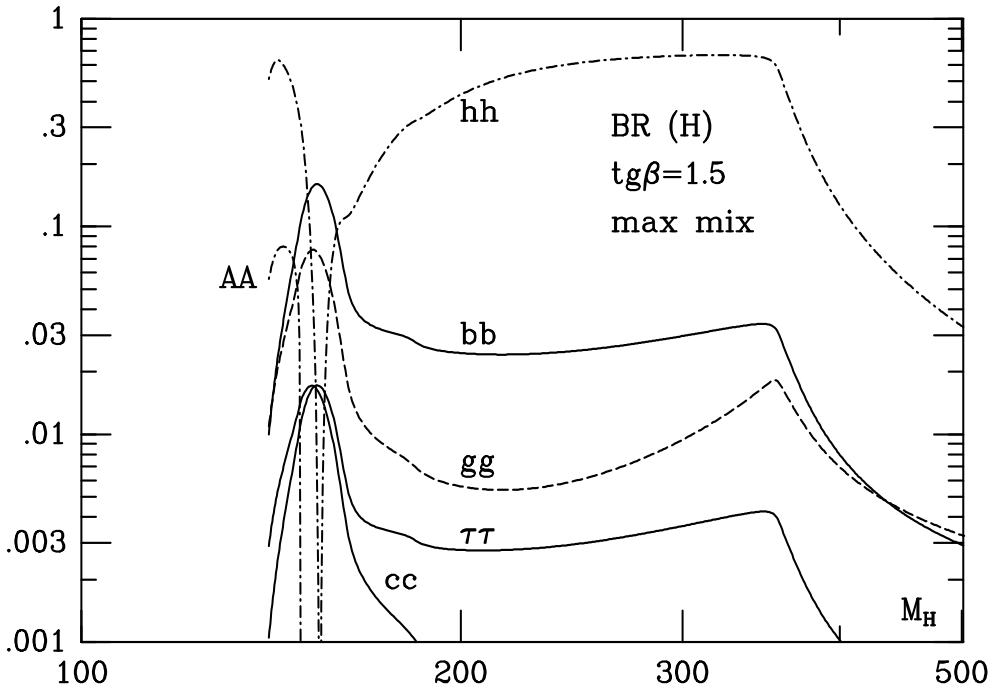
1
.3
.1
.03
.01
.003
.001
100
200
300
500
hh
BR (H)
tgβ=1.5
max mix
AA
bb
gg
ττ
cc
M_H

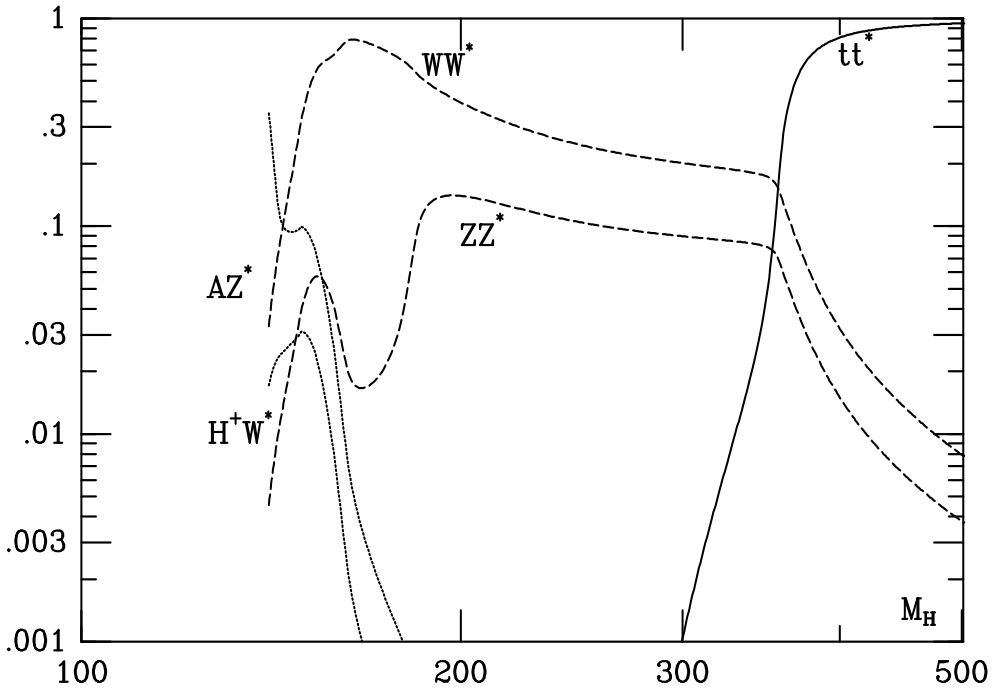
1
.3
.1
.03
.01
.003
.001
100
200
300
500
WW*
tt*
ZZ*
AZ*
H+W*
M_H

Fig. 6b (cont.)

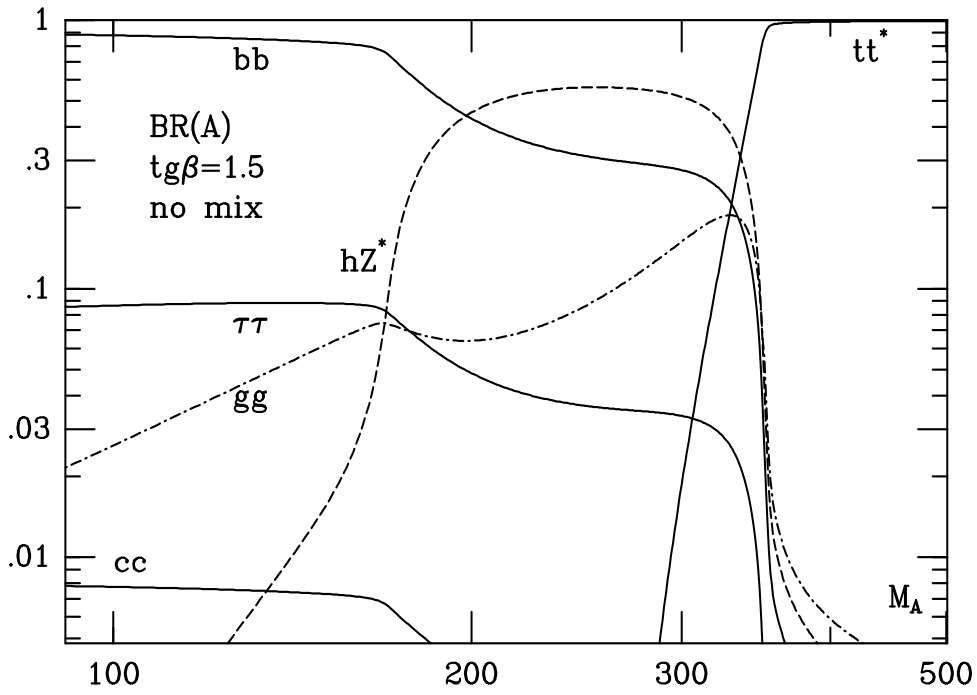
1
.3
.1
.03
.01
bb
tt*
BR(A)
tgβ=1.5
no mix
hZ*
ττ
gg
cc
M_A
100
200
300
500

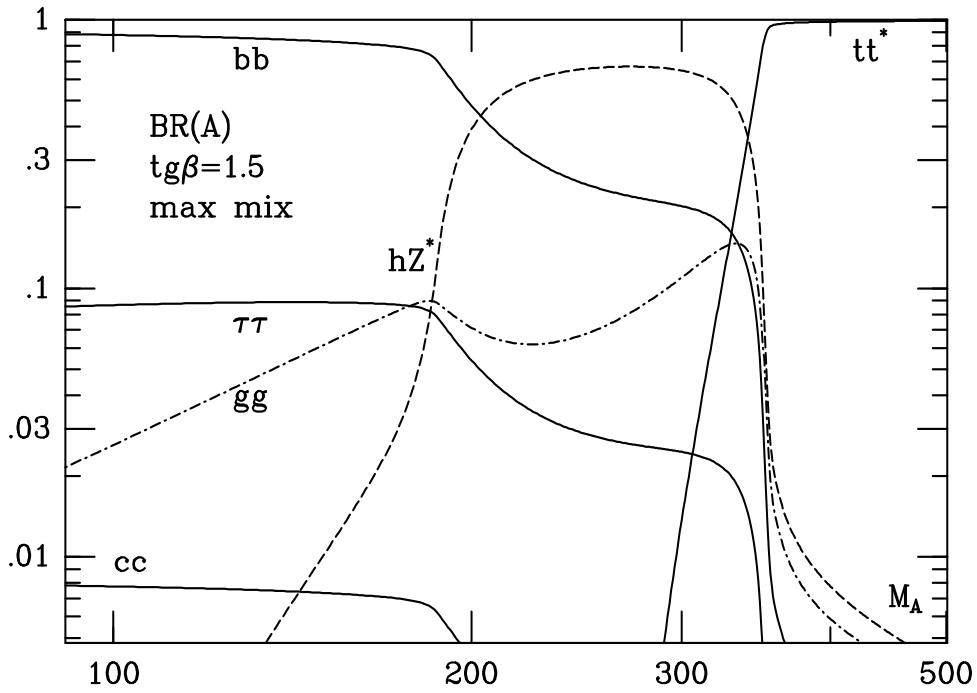
1
.3
.1
.03
.01
bb
tt*
BR(A)
tgβ=1.5
max mix
hZ*
ττ
gg
cc
M_A
100
200
300
500

**Fig. 6c**

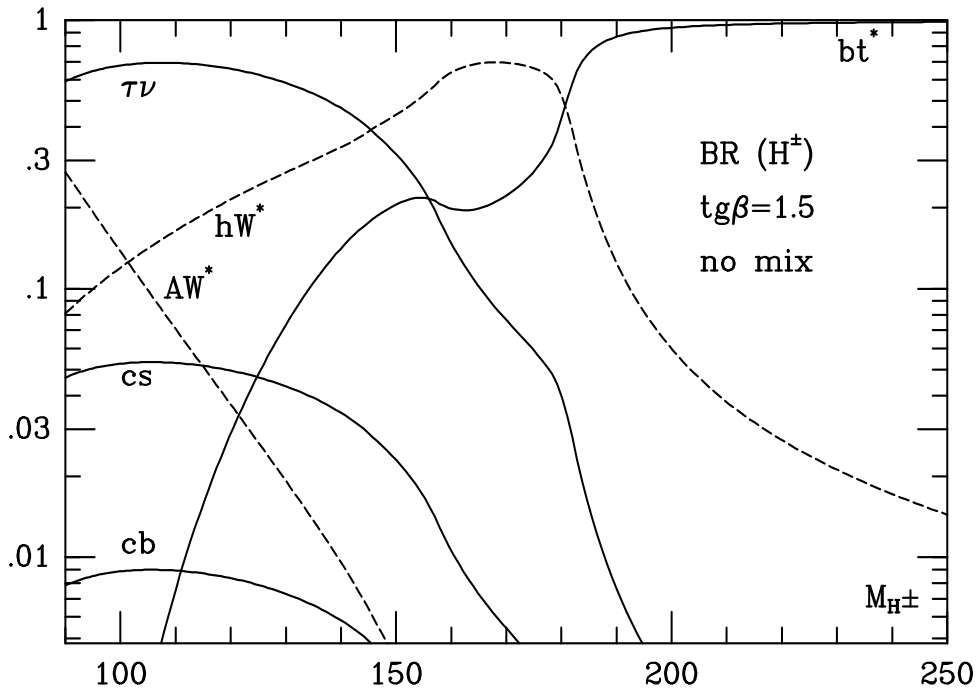
1
.3
.1
.03
.01
100
150
200
250
τν
bt*
hW*
AW*
cs
cb
BR (H±)
tgβ=1.5
no mix
MH±

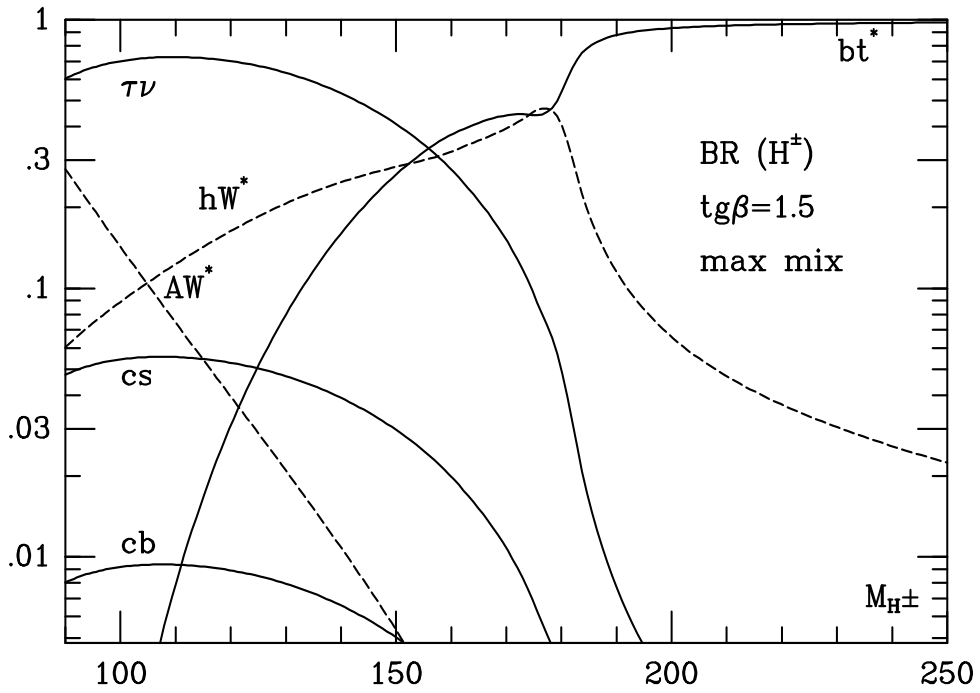
1
.3
.1
.03
.01
100
150
200
250
τν
bt*
hW*
AW*
cs
cb
BR (H±)
tgβ=1.5
max mix
MH±

Fig. 6d

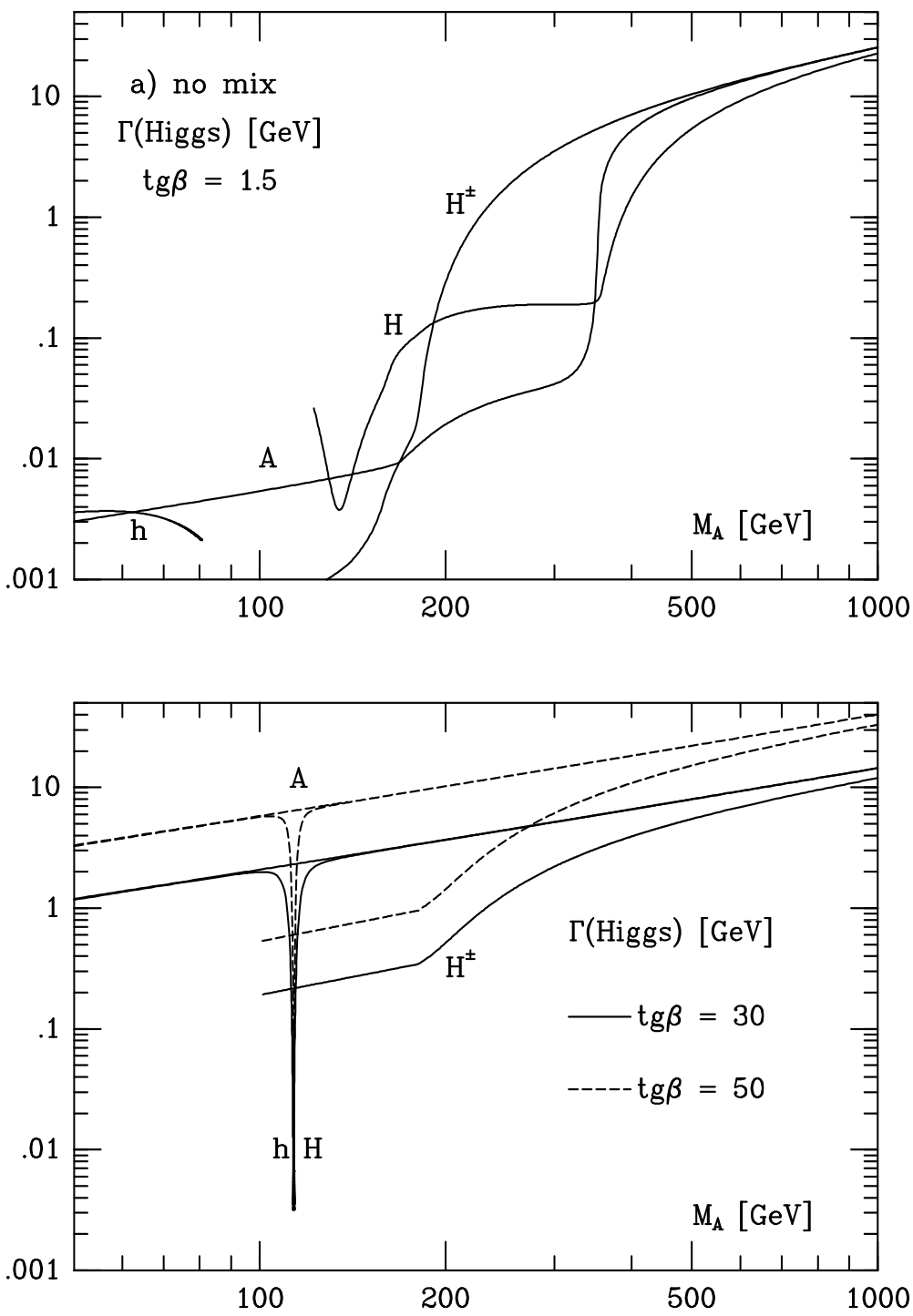
a) no mix
Γ(Higgs) [GeV]
tgβ = 1.5
H±
H
A
h
M_A [GeV]
10
1
.1
.01
.001
100
200
500
1000
A
H±
Γ(Higgs) [GeV]
tgβ = 30
tgβ = 50
h H
M_A [GeV]

Fig. 7

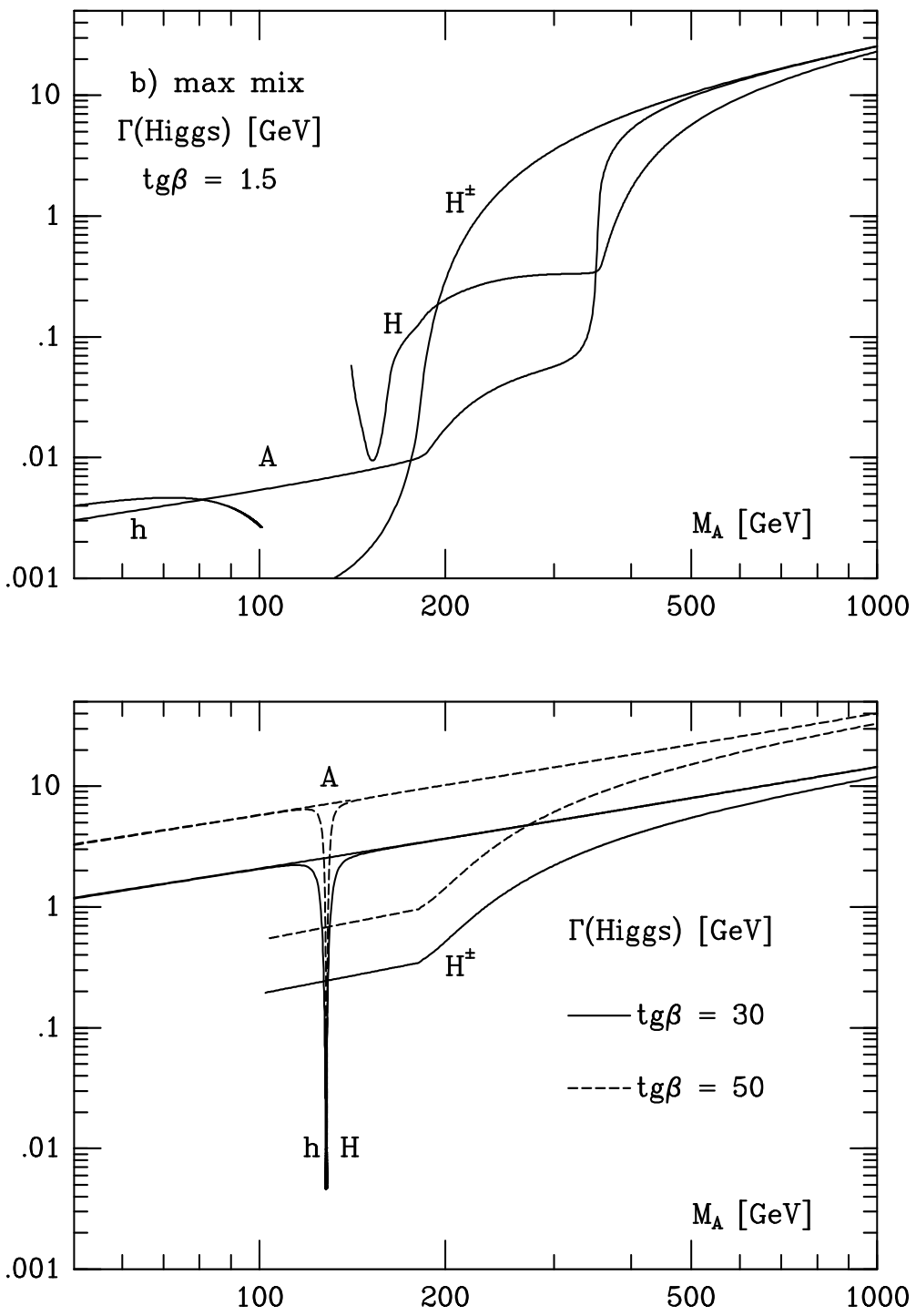
b) max mix
Γ(Higgs) [GeV]
tgβ = 1.5
H±
H
A
h
M_A [GeV]
10
1
.1
.01
.001
100
200
500
1000
A
H±
Γ(Higgs) [GeV]
tgβ = 30
tgβ = 50
h H
M_A [GeV]

Fig. 7 (cont.)